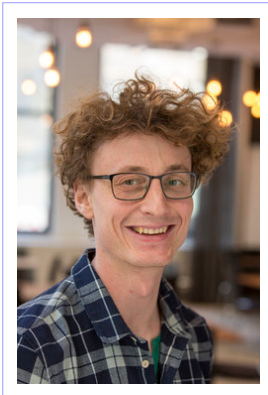


Multiband DMRG real time impurity solver

Hans Gerd Evertz, TU Graz



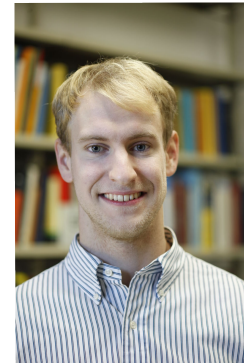
Martin Ganahl



Daniel Bauernfeind



Manuel Zingl



Robert Triebel



Markus Aichhorn

- Hubbard, 2 bands PRB 92, 155132 (2015)
- SrVO_3 3 bands PRX 7, 03101 (2017)
- SrMnO_3 5 bands PRB 97, 115156 (2018)
- Off-diagonal interactions

- Real time: high resolution at all energies
- Can resolve multiplets in Hubbard bands
- As fast as CT-QMC (in cases checked)
- $T=0$
- no sign problems

Outline

- Introduction and brief summary
- Matrix Product States (MPS): the formalism behind DMRG
 - Efficient representations of a state
 - Time evolution
 - Matrix Product Operators and DMRG
- FTPS: new impurity solver
- Results
 - SrVO_3 (3 bands)
 - SrMnO_3 (5 bands)
 - Extensions

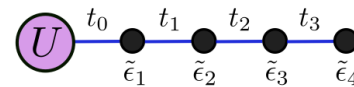
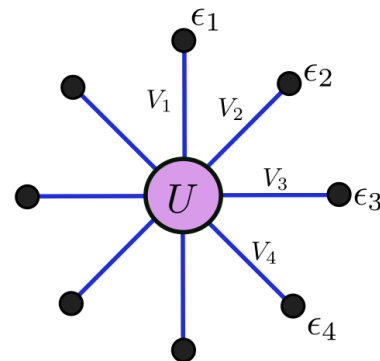
DMFT: task of an impurity solver

Dynamical Mean Field Theory

- Band structure from DFT. Construct local Hamiltonian.
- Difficult task in DMFT cycle:

Calculate Green's function for an Anderson impurity model

$$H_{AIM} = H_{loc} + \sum_k V_k \left(c_k^\dagger c_0 + h.c. \right) + \sum_k \epsilon_k n_k$$



“Star geometry”

\leftrightarrow

Wilson chain

Some current impurity solvers

- **Continuous Time Quantum Monte Carlo (CTQMC):**
 - **Precise** on imaginary axis
 - **Analytic continuation** → **resolution problems, especially at larger energies**
 - Can have **sign problem** and potentially convergence problems
- **Exact Diagonalization (ED) / Configuration interaction (CI)**
 - Exponential Hilbert space (e.g. $N_{\text{bath}} = 3$ for 3 bands)
 - **Low resolution on real frequencies**
- **Numerical Renormalization Group (NRG):**
 - **Real axis**, high resolution at very small energies
 - **Low resolution at larger energies**
- **Matrix Product States (MPS):**
 - DDMRG: high resolution but slow (separate calculation for every ω)
 - Imaginary time: up to 6 orbitals, but few bath sites and low resolution
 - **Real time** → **good resolution at all energies** but **multiband appeared expon. difficult**

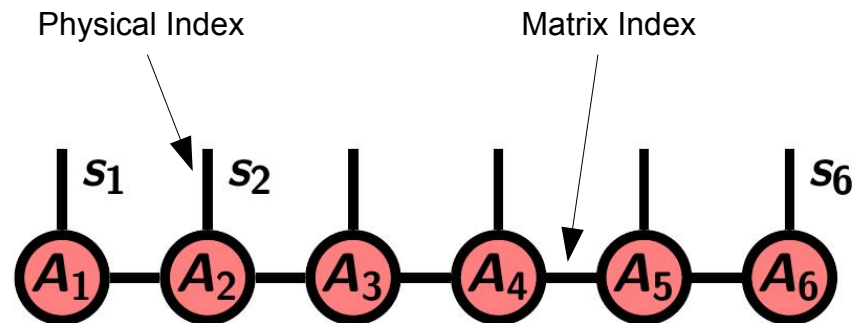
Matrix Product States (MPS)

- Formalism behind DMRG
- **Very efficient representation of states of (mostly) one-dimensional systems:**

$$|\psi\rangle = \sum_{\{s_i\}} \underbrace{c_{s_1, \dots, s_N}}_{= A_1^{s_1} \cdot A_2^{s_2} \dots A_N^{s_N}} |s_1, s_2, \dots, s_N\rangle$$

: Ansatz for coefficients: product of matrices

Graphical representation:



- Ground states by Density Matrix Renormalization Group (DMRG)
Very precise, e.g. **ground state energies exact up to 10 digits** for chains of 100 sites
- Real time evolution, nonequilibrium physics, ...

Real time impurity solvers with MPS: *strategy*

- **To obtain real frequency Green's function:**

- **Calculate ground state** $|\psi_0\rangle$ of impurity model by **DMRG**

- **Time evolve** excitation: $e^{iHt} \underline{c} |\psi_0\rangle$

- Calculate overlap: $G^<(t) = \underline{\langle \psi_0 | c^\dagger} e^{iHt} \underline{c} |\psi_0\rangle$

- “Linear prediction”, Fourier transform $\rightarrow G(\omega)$

Real time impurity solvers with MPS: strategy

- **To obtain real frequency Green's function:**

- **Calculate ground state** $|\psi_0\rangle$ of impurity model by **DMRG**

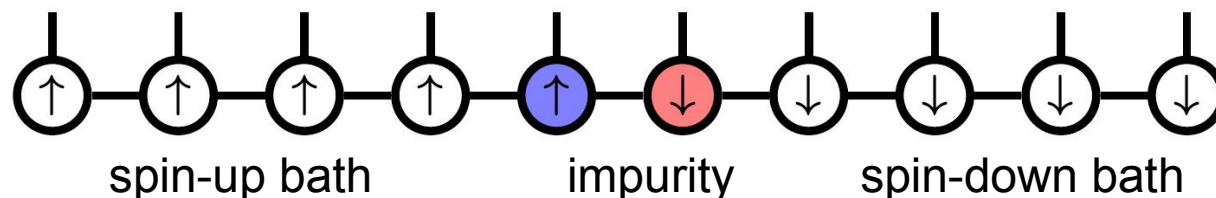
- **Time evolve** excitation: $e^{iHt} \underline{c} |\psi_0\rangle$

- Calculate overlap: $G^<(t) = \underline{\langle \psi_0 | c^\dagger} e^{iHt} \underline{c} |\psi_0\rangle$

- “Linear prediction”, Fourier transform $\rightarrow G(\omega)$

One band:

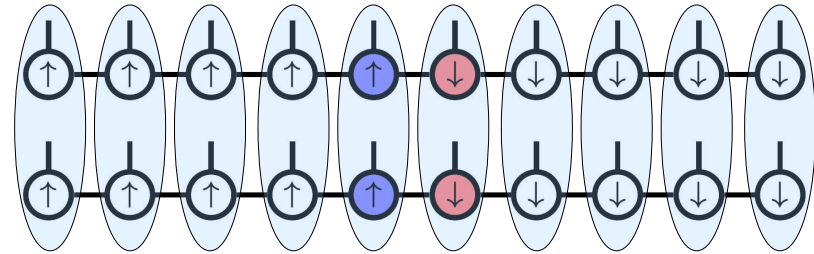
- Separate the spin-up and spin-down baths: (\Rightarrow lower matrix dimensions)



- Large baths ($O(100)$ sites) easily done

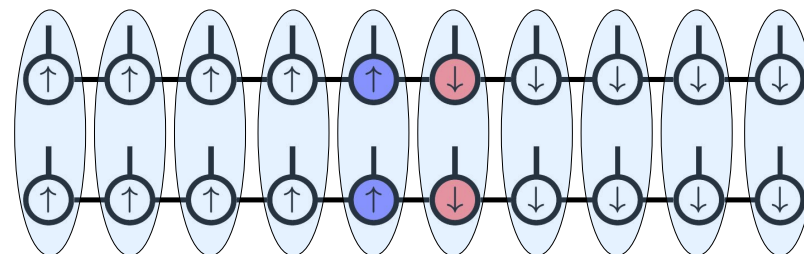
Real time impurity Solver with MPS: two bands

- Combine bands into bigger sites
- Works very well for 2 bands

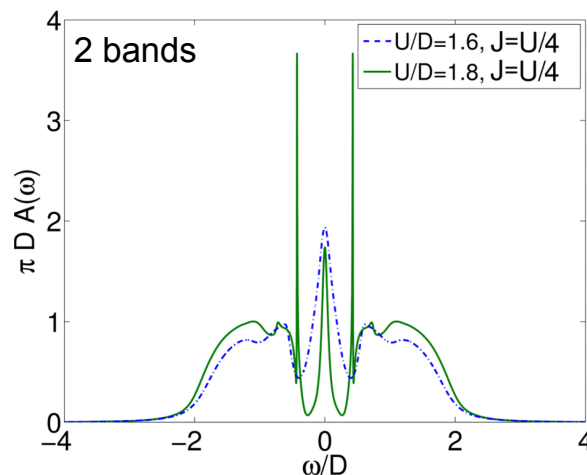
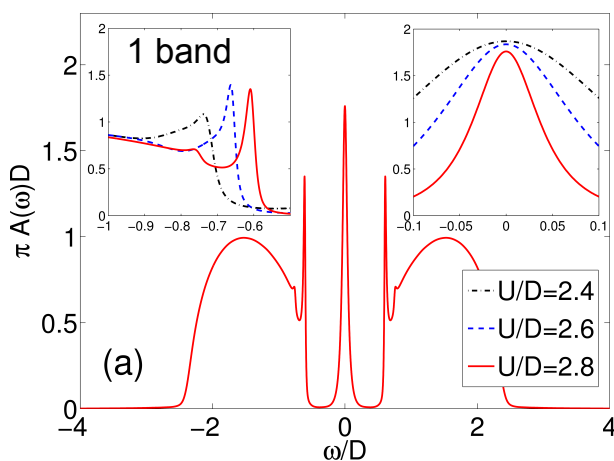


Real time impurity Solver with MPS: two bands

- Combine bands into bigger sites
- Works very well for 2 bands



- Examples: DMFT spectrum of Hubbard model on Bethe lattice (Ganahl et al, 2015)

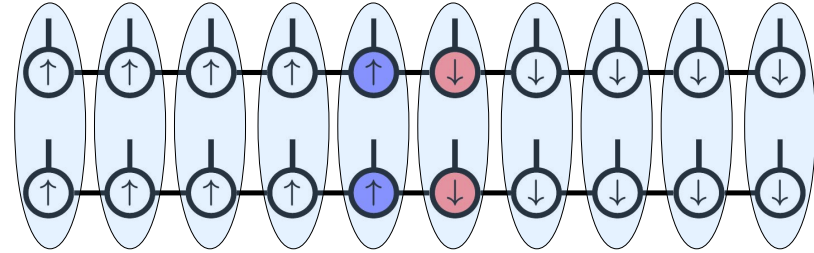


Sharp peaks (invisible in QMC):
from interaction of
doublon-holon pairs

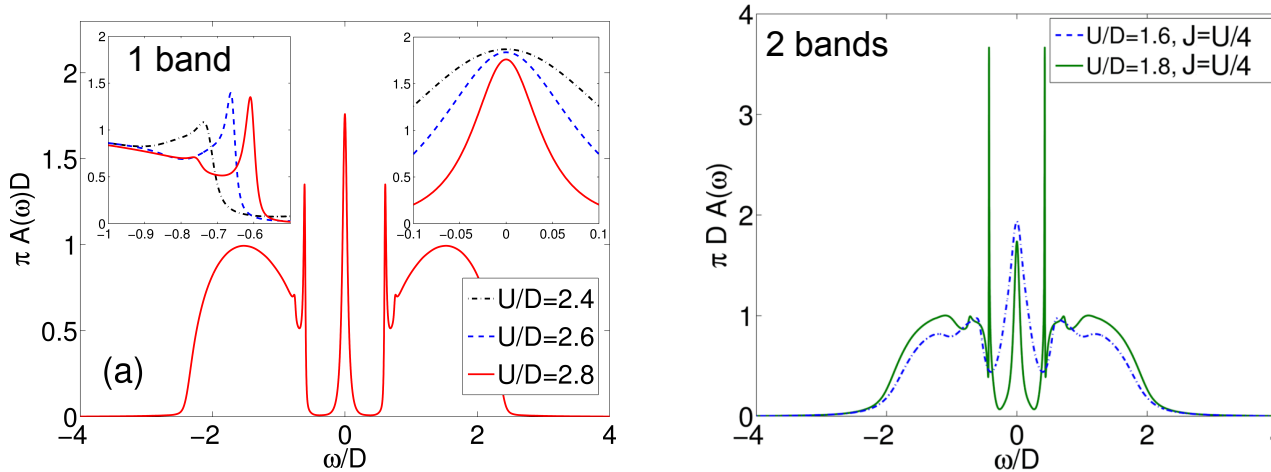
(Lee, von Delft, Weichselbaum,
PRL 2017, one-band model)

Real time impurity Solver with MPS: two bands

- Combine bands into bigger sites
- Works very well for 2 bands



- Examples: DMFT spectrum of Hubbard model on Bethe lattice (Ganahl et al, 2015)



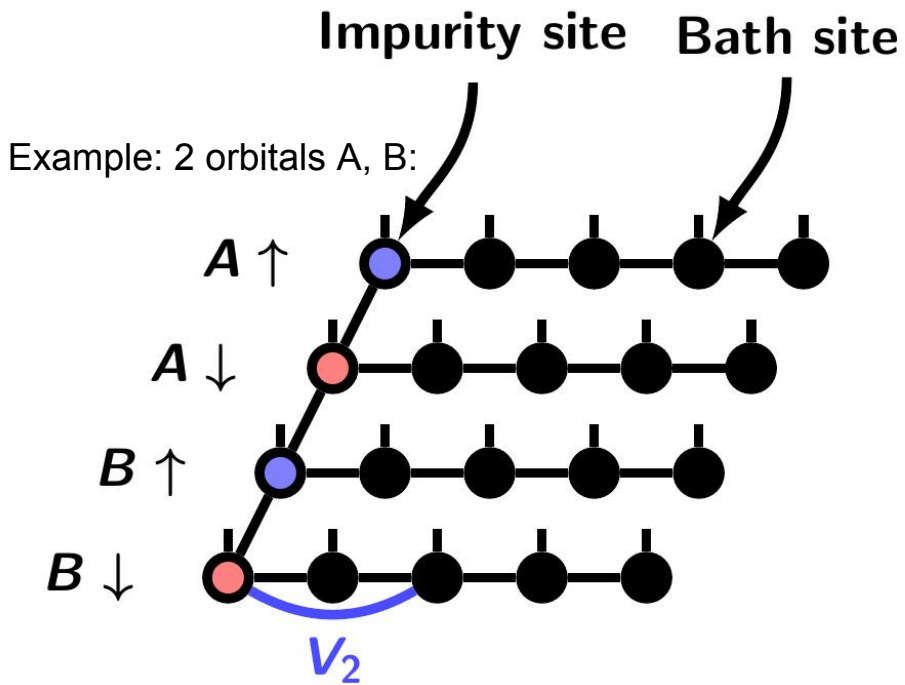
Sharp peaks (invisible in QMC):
from interaction of
doublon-holon pairs

(Lee, von Delft, Weichselbaum,
PRL 2017, one-band model)

- **Problem:** matrix dimensions m multiply: computational effort $\sim m^{3 \times n_bands}$
 \Rightarrow **no more than 2 bands feasible this way**

New approach: Fork Tensor Product States (FTPS)

Bauernfeind 2017, 2018

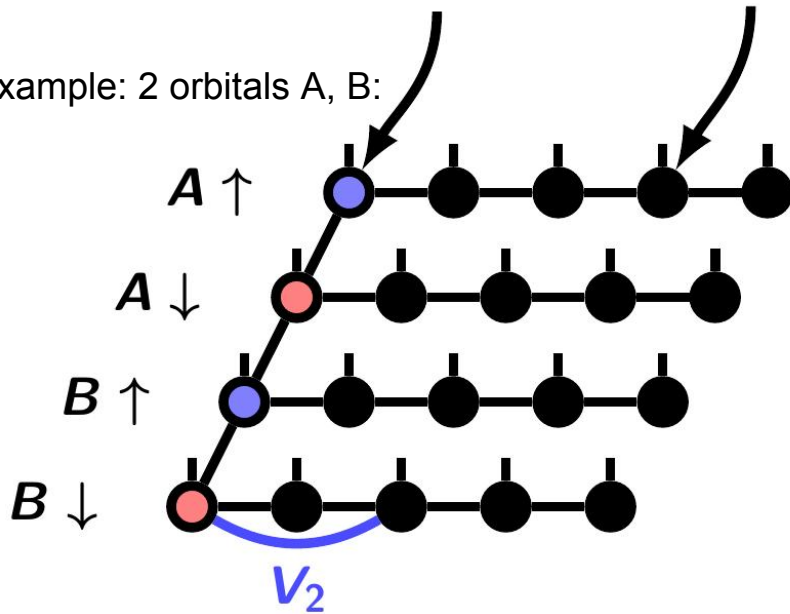


New approach: Fork Tensor Product States (FTPS)

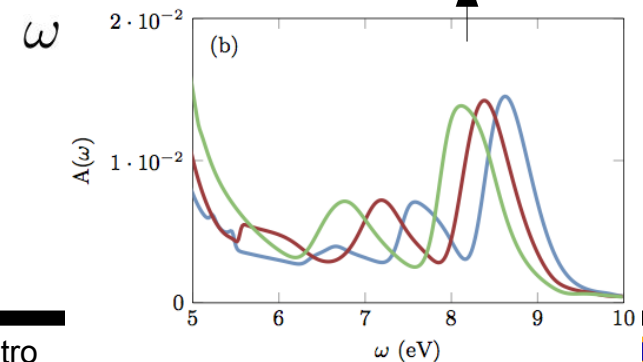
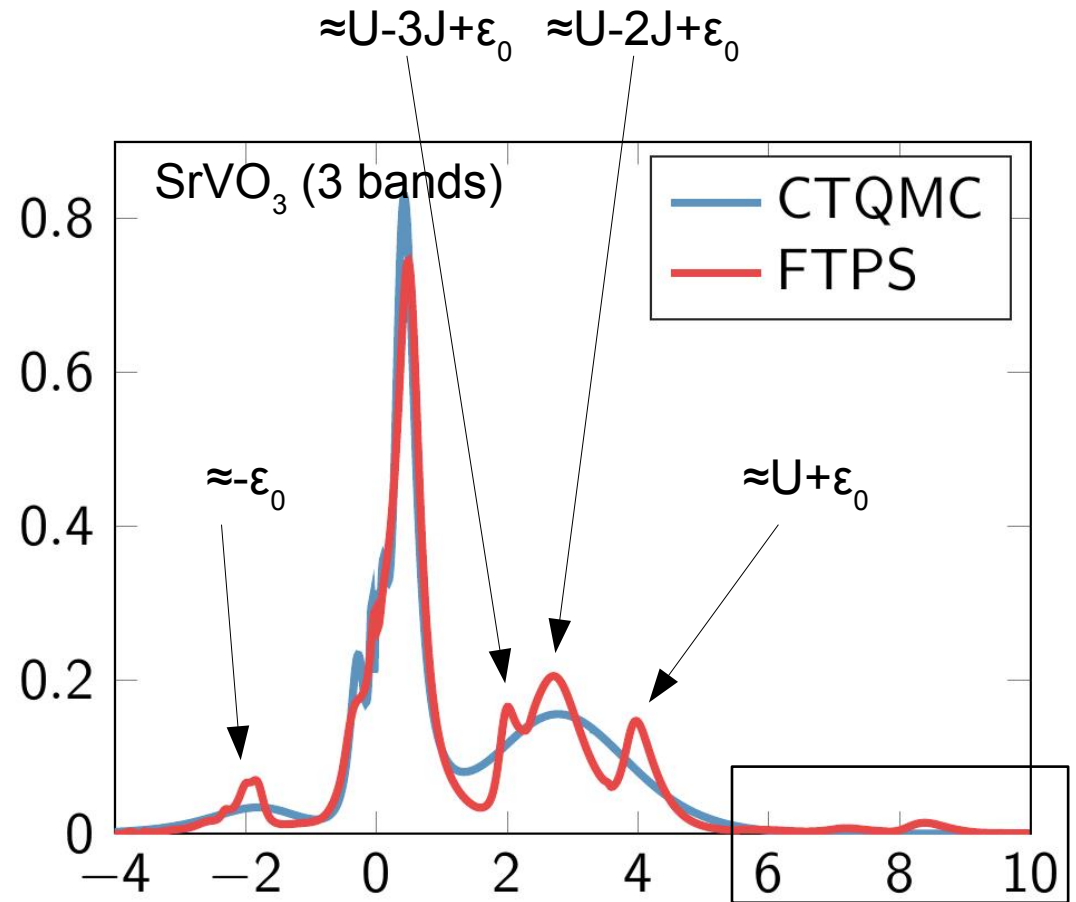
Bauernfeind 2017, 2018

Impurity site Bath site

Example: 2 orbitals A, B:



- Real time: high resolution at all energies
- Can resolve multiplets in Hubbard bands
- As fast as CT-QMC (in cases checked)
- $T=0$
- no sign problems



Matrix Product States

Matrix Product States

Outline:

- **MPS representations of a state**
- **Time evolution**
- **Matrix Product Operators (MPO) and DMRG**

Example: 1d Heisenberg spin chain (equivalent to 1d spinless fermions): 2 states per site

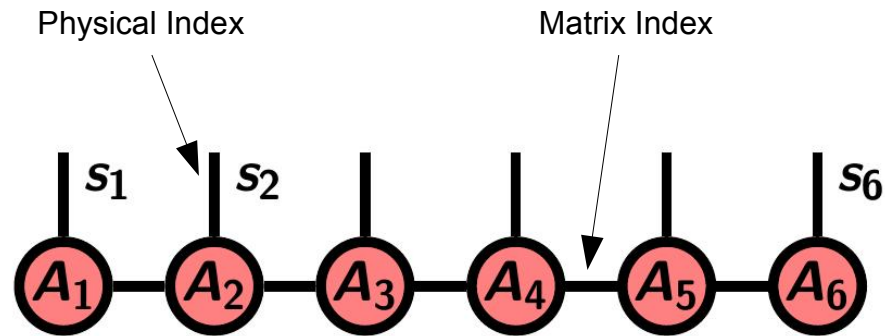
$$\hat{H} = \sum_{i=1}^{L-1} \hat{H}_i \quad \text{with} \quad \hat{H}_i = \frac{J_{xy}}{2} [S_i^+ S_{i+1}^- + S_i^- S_{i+1}^+] + J_z S_i^z S_{i+1}^z$$
$$\Leftrightarrow \hat{H}_i = t (c_j^\dagger c_{j+1} + h.c.) + V (\hat{n}_j - \frac{1}{2})(\hat{n}_{j+1} - \frac{1}{2})$$

MPS representation of a state

- Efficient parametrization of 1d states:

$$|\psi\rangle = \sum_{\{s_i\}} \underbrace{C_{s_1, \dots, s_N}}_{= A_1^{s_1} \cdot A_2^{s_2} \dots A_N^{s_N} : \text{product of matrices}} |s_1, s_2, \dots, s_N\rangle$$

Graphical representation:



Example : (product state)

$ \psi\rangle$	=		↓	↓	↑	↓	↑	↓	>
j	=		1	2	3	4	5	6	
A_j^\uparrow	=		0	0	1	0	1	0	
A_j^\downarrow	=		1	1	0	1	0	1	

MPS representation of a state

Example: (singlet on 2 sites, entangled state)

$$|\psi\rangle = \frac{1}{\sqrt{2}} \left(\begin{array}{c} | \uparrow \quad \downarrow \rangle \\ - | \downarrow \quad \uparrow \rangle \end{array} \right)$$

$$A_j^\uparrow = \begin{pmatrix} 1 & 0 \end{pmatrix}, \quad - \begin{pmatrix} 0 \\ 1 \end{pmatrix} / \sqrt{2}$$

$$A_j^\downarrow = \begin{pmatrix} 0 & 1 \end{pmatrix}, \quad \begin{pmatrix} 1 \\ 0 \end{pmatrix} / \sqrt{2}$$

MPS representation of a state

Example: (singlet on 2 sites, entangled state)

$$|\psi\rangle = \frac{1}{\sqrt{2}} \left(\begin{array}{c} | \uparrow \downarrow \rangle \\ - | \downarrow \uparrow \rangle \end{array} \right)$$

$$A_j^\uparrow = \begin{pmatrix} 1 & 0 \end{pmatrix}, \quad - \begin{pmatrix} 0 \\ 1 \end{pmatrix} / \sqrt{2}$$

$$A_j^\downarrow = \begin{pmatrix} 0 & 1 \end{pmatrix}, \quad \begin{pmatrix} 1 \\ 0 \end{pmatrix} / \sqrt{2}$$

Example: (nonlocal singlet)

$$|\psi\rangle = \frac{1}{\sqrt{2}} \left(\begin{array}{c} | \downarrow \downarrow \uparrow \downarrow \downarrow \downarrow \downarrow \downarrow \downarrow \rangle \\ - | \downarrow \downarrow \downarrow \uparrow \downarrow \downarrow \downarrow \downarrow \downarrow \rangle \end{array} \right)$$

$$A_j^\uparrow = \begin{matrix} 0, & 0, & (1, 0), & \begin{pmatrix} 0 & 0 \\ 0 & 0 \end{pmatrix}, & \begin{pmatrix} 0 & 0 \\ 0 & 0 \end{pmatrix}, & - \begin{pmatrix} 0 \\ 1 \end{pmatrix} / \sqrt{2}, & 0, & 0 \end{matrix}$$

$$A_j^\downarrow = \begin{matrix} 1, & 1, & (0, 1), & \begin{pmatrix} 1 & 0 \\ 0 & 1 \end{pmatrix}, & \begin{pmatrix} 1 & 0 \\ 0 & 1 \end{pmatrix}, & \begin{pmatrix} 1 \\ 0 \end{pmatrix} / \sqrt{2}, & 1, & 1 \end{matrix}$$

Main tool: Singular Value Decomposition (SVD)

- Every $m \times n$ matrix M can be decomposed as

$$\text{e.g.: } \boxed{M} = \boxed{U} \boxed{D} \boxed{V^\dagger}$$

$$M = U D V^\dagger$$

with $U^\dagger U = 1$ and $V^\dagger V = 1$

- D is diagonal and contains r positive singular values

$$\lambda_1 \geq \lambda_2 \geq \dots \geq \lambda_r > \lambda_{r+1} = 0 = \dots = \lambda_N = 0$$

$$D = \begin{pmatrix} \lambda_1 & & & & & \\ & \ddots & & & & \\ & & \lambda_r & & & \\ & & & 0 & & \\ & & & & \ddots & \\ & & & & & 0 \end{pmatrix}$$

- SVD is very useful to approximate a matrix by neglecting small singular values

(e.g. image compression, signal compression) Computational effort $O(\min(mn^2, m^2n))$

Main tool: Singular Value Decomposition (SVD)

- Every $m \times n$ matrix M can be decomposed as

$$\text{e.g.: } \boxed{M} = \boxed{U} \boxed{D} \boxed{V^\dagger}$$

$$M = U D V^\dagger$$

with $U^\dagger U = 1$ and $V^\dagger V = 1$

- D is diagonal and contains r positive singular values

$$\lambda_1 \geq \lambda_2 \geq \dots \geq \lambda_r > \lambda_{r+1} = 0 = \dots = \lambda_N = 0$$

$$D = \begin{pmatrix} \lambda_1 & & & & & \\ & \ddots & & & & \\ & & \lambda_r & & & \\ & & & 0 & & \\ & & & & \ddots & \\ & & & & & 0 \end{pmatrix}$$

- SVD is very useful to approximate a matrix by neglecting small singular values

(e.g. image compression, signal compression; computational effort $O(\min(mn^2, m^2n))$)

- SVD version with unitary matrices: $M = \tilde{U} \tilde{D} \tilde{V}^\dagger$

$$\boxed{M} = \boxed{U} \boxed{D \text{ --- } 0 \ 0 \ 0} \begin{array}{|c|} \hline V^\dagger \\ \hline \text{(rest)} \\ \hline \end{array}$$

Lower rows of \tilde{V}^\dagger do not contribute to M because of the zeroes in \tilde{D} . They belong to the null space of M .

Tool: Schmidt decomposition of a state

- Divide a system arbitrarily into parts A and B



- **Generic state**

$$|\Psi\rangle = \sum_{j,k} c_{jk} |j\rangle_A |k\rangle_B$$

- **SVD of the coefficients:**

$$(c_{jk}) = \tilde{U} \tilde{D} \tilde{V}^\dagger$$

- \rightarrow **basis transformation** $|A\rangle_\alpha := \sum_j \tilde{U}_{j\alpha} |j\rangle_A$, $|B\rangle_\alpha := \sum_k (\tilde{V}^\dagger)_{\alpha k} |k\rangle_B$

- \rightarrow Schmidt decomposition

$$|\Psi\rangle = \sum_{\alpha=1}^{\chi} \lambda_\alpha |A\rangle_\alpha |B\rangle_\alpha$$

“diagonal” singular values λ_α

$$\text{with } \chi \leq \min(\dim(A), \dim(B)) \quad \text{and} \quad \sum_{\alpha} \lambda_\alpha^2 = 1.$$

Entanglement between subsystems A and B



- When operator \hat{O} acts only on A :

$$\langle \psi | \hat{O} | \psi \rangle = \sum_{\alpha\beta} \lambda_{\alpha} \lambda_{\beta} \langle B |_{\alpha} \langle A | \hat{O} | A \rangle_{\beta} | B \rangle_{\beta} = \sum_{\alpha} \lambda_{\alpha}^2 \langle A | \hat{O} | A \rangle_{\alpha}$$

$$= \text{tr}_A \left(\hat{O} \underbrace{\sum_{\alpha} \lambda_{\alpha}^2 |A\rangle_{\alpha} \langle A|}_{\hat{\rho}_A} \right)$$

$\hat{\rho}_A$: reduced density matrix = $\text{tr}_B \hat{\rho} \equiv \text{tr}_B |\psi\rangle \langle \psi|$

Entanglement between subsystems A and B



- When operator \hat{O} acts only on A :

$$\langle \psi | \hat{O} | \psi \rangle = \sum_{\alpha\beta} \lambda_{\alpha} \lambda_{\beta} \langle B |_{\alpha} \langle A | \hat{O} | A \rangle_{\beta} | B \rangle_{\beta} = \sum_{\alpha} \lambda_{\alpha}^2 \langle A | \hat{O} | A \rangle_{\alpha}$$

$$= \text{tr}_A \left(\hat{O} \underbrace{\sum_{\alpha} \lambda_{\alpha}^2 |A\rangle_{\alpha} \langle A|}_{\hat{\rho}_A} \right)$$

$\hat{\rho}_A$: reduced density matrix = $\text{tr}_B \hat{\rho} \equiv \text{tr}_B |\psi\rangle \langle \psi|$

Von Neumann entanglement entropy between A and B :

$$S_A := - \text{tr}_A (\hat{\rho}_A \ln \hat{\rho}_A) = - \sum_{\alpha} \lambda_{\alpha}^2 \ln \lambda_{\alpha}^2 \quad \text{depends only on } \lambda_{\alpha}$$

Entanglement between subsystems A and B



- When operator O acts only on A :

$$\langle \psi | \hat{O} | \psi \rangle = \sum_{\alpha\beta} \lambda_{\alpha} \lambda_{\beta} \langle B |_{\alpha} \langle A | \hat{O} | A \rangle_{\beta} | B \rangle_{\beta} = \sum_{\alpha} \lambda_{\alpha}^2 \langle A | \hat{O} | A \rangle_{\alpha}$$

$$= \text{tr}_A \left(\hat{O} \underbrace{\sum_{\alpha} \lambda_{\alpha}^2 |A\rangle_{\alpha} \langle A|}_{\hat{\rho}_A} \right)$$

$\hat{\rho}_A$: reduced density matrix = $\text{tr}_B \hat{\rho} \equiv \text{tr}_B |\psi\rangle \langle \psi|$

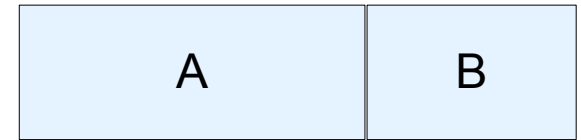
- Von Neumann entanglement entropy between A and B :

$$S_A := - \text{tr}_A(\hat{\rho}_A \ln \hat{\rho}_A) = - \sum_{\alpha} \lambda_{\alpha}^2 \ln \lambda_{\alpha}^2 \quad \text{depends only on } \lambda_{\alpha}$$

- Maximum possible value: $S_{A,max} = \ln \chi$ (when all λ_{α} are equal)

→ need matrices up to dimension $\chi \simeq \exp(S_A)$

Entanglement between subsystems A and B



- When operator O acts only on A :

$$\langle \psi | \hat{O} | \psi \rangle = \sum_{\alpha\beta} \lambda_{\alpha} \lambda_{\beta} \langle B |_{\alpha} \langle A | \hat{O} | A \rangle_{\beta} | B \rangle_{\beta} = \sum_{\alpha} \lambda_{\alpha}^2 \langle A | \hat{O} | A \rangle_{\alpha}$$

$$= \text{tr}_A \left(\hat{O} \underbrace{\sum_{\alpha} \lambda_{\alpha}^2 |A\rangle_{\alpha} \langle A|}_{\hat{\rho}_A} \right)$$

$\hat{\rho}_A$: reduced density matrix = $\text{tr}_B \hat{\rho} \equiv \text{tr}_B |\psi\rangle \langle \psi|$

- Von Neumann entanglement entropy between A and B :

$$S_A := - \text{tr}_A (\hat{\rho}_A \ln \hat{\rho}_A) = - \sum_{\alpha} \lambda_{\alpha}^2 \ln \lambda_{\alpha}^2 \quad \text{depends only on } \lambda_{\alpha}$$

- Maximum possible value: $S_{A,max} = \ln \chi$ (when all λ_{α} are equal)

→ need matrices up to dimension $\chi \simeq \exp(S_A)$

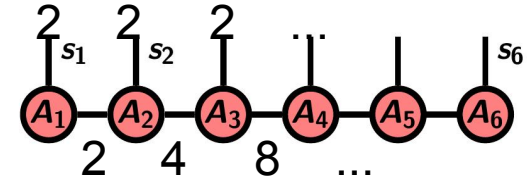
- Examples: Product state: $|\Psi\rangle = |\uparrow_A \uparrow_B\rangle = |\uparrow\rangle_A |\uparrow\rangle_B$: $S_A = 0$: not entangled

$$\text{Singlet: } |\Psi\rangle = \frac{1}{\sqrt{2}} (|\uparrow\rangle_A |\downarrow\rangle_B - |\uparrow\rangle_B |\downarrow\rangle_A) : S_A = \ln 2 : \text{max. entangled}$$

Exact MPS representation of a state

- General state:

$$|\Psi\rangle = \sum_{s_1 \dots s_L} c_{s_1 \dots s_L} |s_1 \dots s_L\rangle$$



First site: SVD

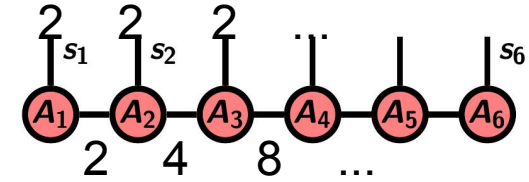
$$c_{s_1, (s_2 \dots s_L)} = \sum_{\alpha_1=1}^2 \underbrace{\tilde{U}_{s_1 \alpha_1}^{[1]}}_{2 \times 2 \text{ matrix}} \lambda_{\alpha_1}^{[1]} \tilde{V}_{\alpha_1 (s_2 \dots s_L)}^\dagger(0)$$

with singular values λ_{α_1}

Also gives Schmidt decomposition between sites 1 and 2

Exact MPS representation of a state

- General state:
$$|\Psi\rangle = \sum_{s_1 \dots s_L} c_{s_1 \dots s_L} |s_1 \dots s_L\rangle$$

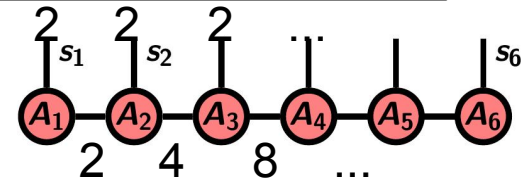


- First site: SVD
$$c_{s_1, (s_2 \dots s_L)} = \sum_{\alpha_1=1}^2 \underbrace{\tilde{U}_{s_1 \alpha_1}^{[1]}}_{2 \times 2 \text{ matrix}} \lambda_{\alpha_1}^{[1]} \tilde{V}_{\alpha_1 (s_2 \dots s_L)}^\dagger(0)$$
 with singular values λ_{α_1}

Also gives Schmidt decomposition between sites 1 and 2

- Second site: SVD
$$\lambda_{\alpha_1} \tilde{V}_{\alpha_1 (s_2 \dots s_L)}^\dagger = \sum_{\alpha_2=1}^4 \underbrace{\tilde{U}_{(\alpha_1 s_2) \alpha_2}^{[2]}}_{4 \times 4 \text{ matrix}} \lambda_{\alpha_2}^{[2]} \tilde{V}_{\alpha_2 (s_3 \dots s_L)}^\dagger$$
 with singular values λ_{α_2}

Exact MPS representation of a state



- General state:
$$|\Psi\rangle = \sum_{s_1 \dots s_L} c_{s_1 \dots s_L} |s_1 \dots s_L\rangle$$

- First site: SVD
$$c_{s_1, (s_2 \dots s_L)} = \sum_{\alpha_1=1}^2 \underbrace{\tilde{U}_{s_1 \alpha_1}^{[1]}}_{2 \times 2 \text{ matrix}} \lambda_{\alpha_1}^{[1]} \tilde{V}_{\alpha_1 (s_2 \dots s_L)}^\dagger(0)$$
 with singular values λ_{α_1}

Also gives Schmidt decomposition between sites 1 and 2

- Second site: SVD
$$\lambda_{\alpha_1} \tilde{V}_{\alpha_1 (s_2 \dots s_L)}^\dagger = \sum_{\alpha_2=1}^4 \underbrace{\tilde{U}_{(\alpha_1 s_2) \alpha_2}^{[2]}}_{4 \times 4 \text{ matrix}} \lambda_{\alpha_2}^{[2]} \tilde{V}_{\alpha_2 (s_3 \dots s_L)}^\dagger$$
 with singular values λ_{α_2}

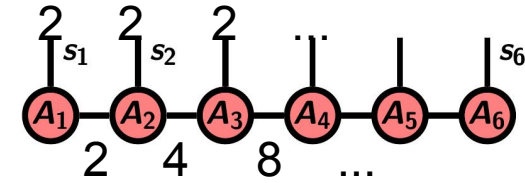
- After site j:
$$|\Psi\rangle = \sum_{s_1 \dots s_L} \sum_{\alpha_1}^2 \sum_{\alpha_2}^4 \sum_{\alpha_3}^8 \dots U_{s_1 \alpha_1}^{[1]} U_{(\alpha_1 s_2) \alpha_2}^{[2]} \dots U_{(\alpha_{j-1} s_j) \alpha_j}^{[j]} \lambda_{\alpha_j}^{[j]} V_{\alpha_j (s_{j+1} \dots s_L)}^\dagger |s_1 \dots s_L\rangle$$

- Rename U \rightarrow A:
$$U_{s_1 \alpha_1}^{[1]} U_{(\alpha_1 s_2) \alpha_2}^{[2]} U_{(\alpha_2 s_3) \alpha_3}^{[3]} \dots =: A_{\alpha_1}^{[1] s_1} A_{\alpha_1 \alpha_2}^{[2] s_2} A_{\alpha_2 \alpha_3}^{[3] s_3} \dots$$

- \rightarrow Exact MPS:
$$|\Psi\rangle = \sum_{s_1 \dots s_L} \sum_{\{\alpha_i\}} A_{\alpha_1}^{[1] s_1} A_{\alpha_1 \alpha_2}^{[2] s_2} A_{\alpha_2 \alpha_3}^{[3] s_3} \dots A_{\alpha_{L-2} \alpha_{L-1}}^{[L-1] s_{L-1}} A_{\alpha_{L-1}}^{[L] s_L} |s_1 \dots s_L\rangle$$

Exact MPS representation of a state

- General state:
$$|\Psi\rangle = \sum_{s_1 \dots s_L} c_{s_1 \dots s_L} |s_1 \dots s_L\rangle$$



- First site: SVD
$$c_{s_1(s_2 \dots s_L)} = \sum_{\alpha_1=1}^2 \underbrace{\tilde{U}_{s_1 \alpha_1}^{[1]}}_{2 \times 2 \text{ matrix}} \lambda_{\alpha_1}^{[1]} \tilde{V}_{\alpha_1(s_2 \dots s_L)}^\dagger(0)$$
 with singular values λ_{α_1}

Also gives Schmidt decomposition between sites 1 and 2

- Second site: SVD
$$\lambda_{\alpha_1} \tilde{V}_{\alpha_1(s_2 \dots s_L)}^\dagger = \sum_{\alpha_2=1}^4 \underbrace{\tilde{U}_{(\alpha_1 s_2) \alpha_2}^{[2]}}_{4 \times 4 \text{ matrix}} \lambda_{\alpha_2}^{[2]} \tilde{V}_{\alpha_2(s_3 \dots s_L)}^\dagger$$
 with singular values λ_{α_2}

- After site j:
$$|\Psi\rangle = \sum_{s_1 \dots s_L} \sum_{\alpha_1}^2 \sum_{\alpha_2}^4 \sum_{\alpha_3}^8 \dots U_{s_1 \alpha_1}^{[1]} U_{(\alpha_1 s_2) \alpha_2}^{[2]} \dots U_{(\alpha_{j-1} s_j) \alpha_j}^{[j]} \lambda_{\alpha_j}^{[j]} V_{\alpha_j(s_{j+1} \dots s_L)}^\dagger |s_1 \dots s_L\rangle$$

- Rename U \rightarrow A :
$$U_{s_1 \alpha_1}^{[1]} U_{(\alpha_1 s_2) \alpha_2}^{[2]} U_{(\alpha_2 s_3) \alpha_3}^{[3]} \dots =: A_{\alpha_1}^{[1]s_1} A_{\alpha_1 \alpha_2}^{[2]s_2} A_{\alpha_2 \alpha_3}^{[3]s_3} \dots$$

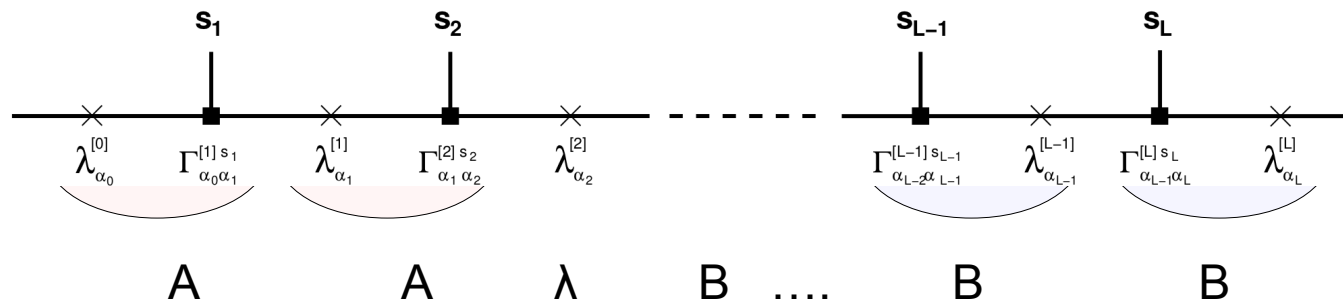
- \rightarrow Exact MPS:
$$|\Psi\rangle = \sum_{s_1 \dots s_L} \sum_{\{\alpha_i\}} A_{\alpha_1}^{[1]s_1} A_{\alpha_1 \alpha_2}^{[2]s_2} A_{\alpha_2 \alpha_3}^{[3]s_3} \dots A_{\alpha_{L-2} \alpha_{L-1}}^{[L-1]s_{L-1}} A_{\alpha_{L-1}}^{[L]s_L} |s_1 \dots s_L\rangle$$

- But: **maximum dimension $2^{L/2}$** (!?!) in the middle (by doing SVD from left and from right)
Really: matrix dimensions **O(100)** are enough! (see later)

Canonical representation and normalization

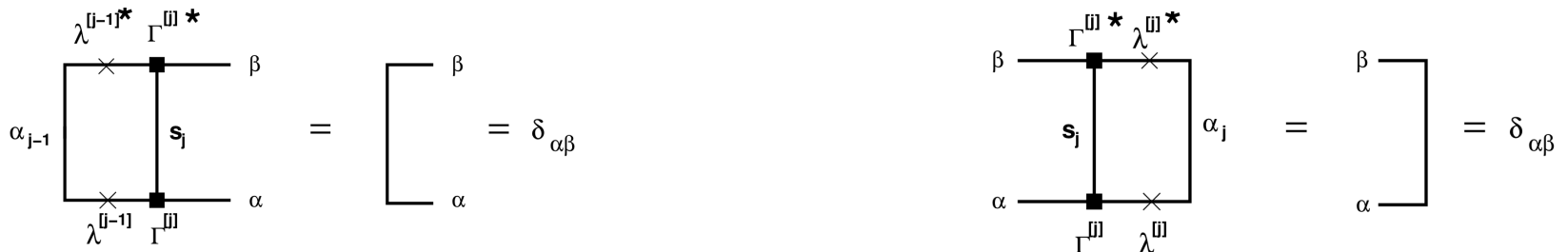
- Write singular values explicitly, by defining matrices Γ :

$$A_{\alpha_{j-1} \alpha_j}^{[j] s_j} =: \lambda_{\alpha_{j-1}}^{[j-1]} \Gamma_{\alpha_{j-1} \alpha_j}^{[j] s_j} \quad \text{and also} \quad B_{\alpha_{j-1} \alpha_j}^{[j] s_j} := \Gamma_{\alpha_{j-1} \alpha_j}^{[j] s_j} \lambda_{\alpha_j}^{[j]}$$



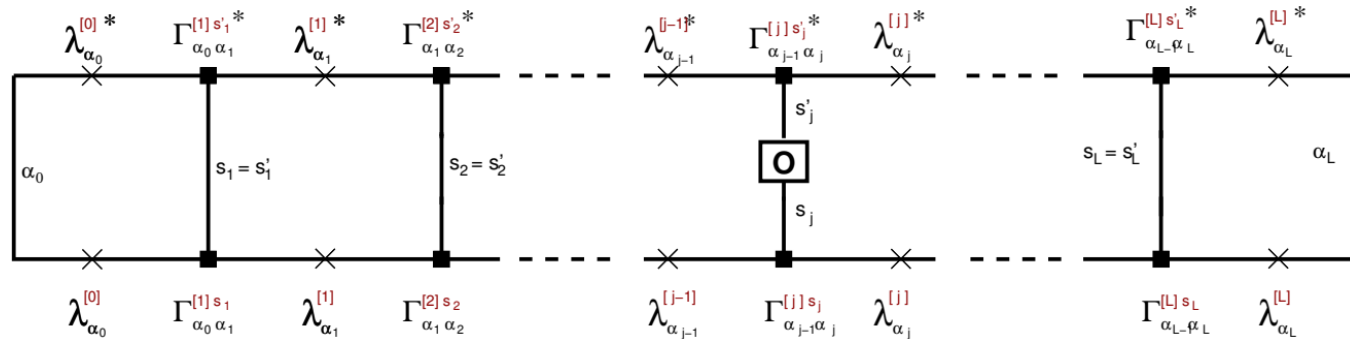
Provides Schmidt decomp. and reduced density matrix at any lattice bond

- Normalization: write $U^\dagger U = 1$ and $V^\dagger V = 1$ graphically:

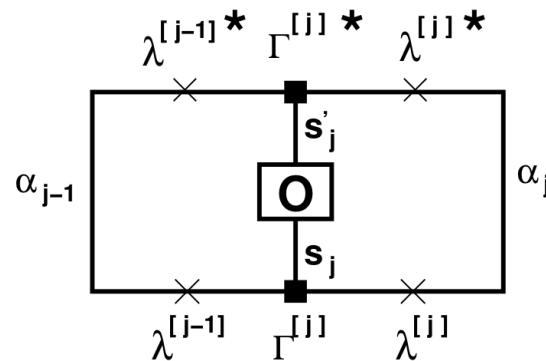


Expectation value of a local operator

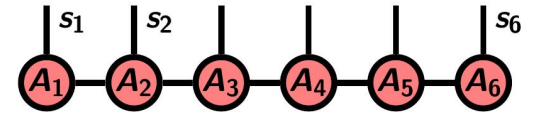
$$\langle \Psi | \hat{O}^{[j]} | \Psi \rangle = \sum_{\{s\}, \{s'\}} \langle s'_1 \dots s'_L | \dots \lambda^{*[j]} \Gamma^{*[j]} s'_j \lambda^{*[j-1]} \dots O_{s_j s'_j}^{[j]} \dots \lambda^{[j-1]} \Gamma^{[j]} s_j \lambda^{[j]} \dots | s_1 \dots s_L \rangle$$



Simplifies because of normalizations and becomes a *local* object



For 1d chains, **small** matrices are enough !



- In 1D, entanglement between “left” and “right” subsystem goes through a single bond
→ entanglement entropy S is small, up to only $\ln(\text{system size } N)$ (*for ground states*)
→ need only matrix dimensions $\chi = O(N) = O(100)$
- But excited states (time evolution) may need much more
- In higher dimensions: $S_{max} \sim L^{D-1} \rightarrow$ exponentially large matrices
- In practice, **truncate matrices** by discarding small singular values,
either to a maximum size (uncontrolled error),
or by limiting the “truncated weight” $t_w := \sum_{\alpha} \lambda_{\alpha}^2$ of the discarded directions to e.g. 10^{-10}

Time evolution

- H with nearest neighbor coupling: split $\hat{H} = \hat{H}_{even} + \hat{H}_{odd} = \sum_{j,odd} \hat{H}_j + \sum_{j,even} \hat{H}_j$

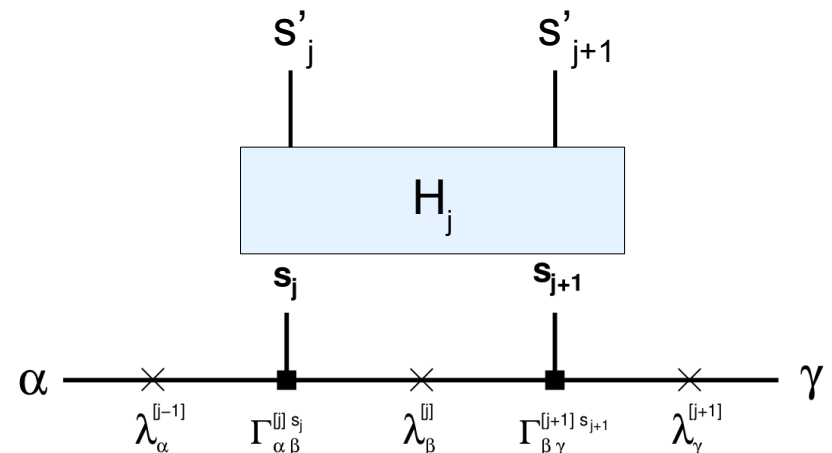
such that $e^{-i\hat{H}_{even}t} = \prod_{j,even} e^{-i\hat{H}_j t}$ and $e^{-i\hat{H}_{odd}t} = \prod_{j,odd} e^{-i\hat{H}_j t}$

2-site operators

- Trotter-Suzuki:** $e^{-i\hat{H}t} = \left(e^{-i\hat{H}_{even}\Delta t} e^{-i\hat{H}_{odd}\Delta t} e^{-i\hat{H}_{even}\Delta t} \dots e^{-i\hat{H}_{even}\Delta t} \right) (1 + \mathcal{O}(\Delta t))$

(other operator sequences are possible)

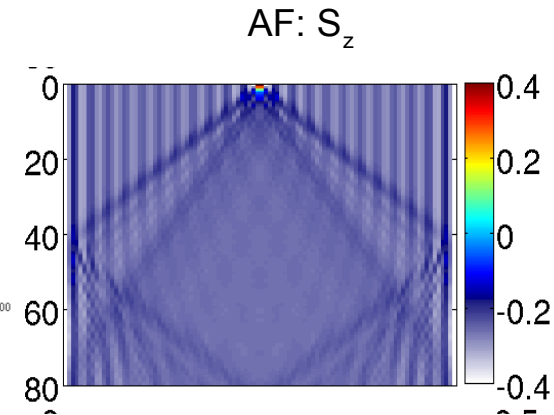
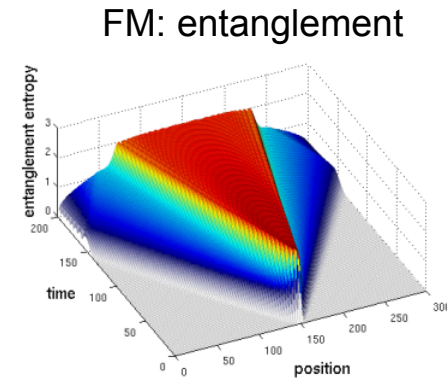
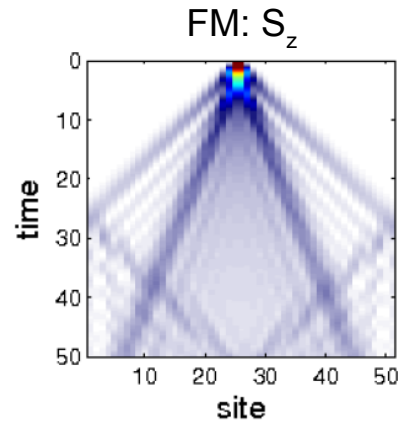
- 2-site operators can be applied locally



- Matrix dimensions would double at each step \rightarrow truncate back

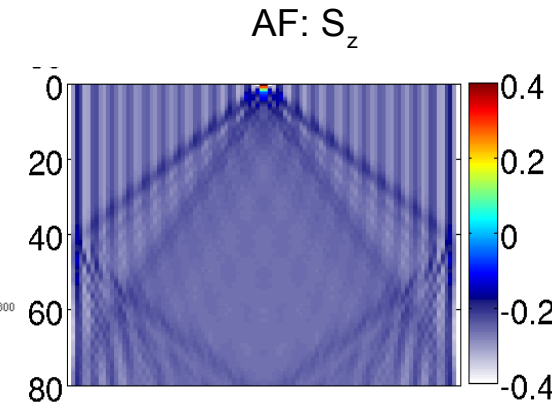
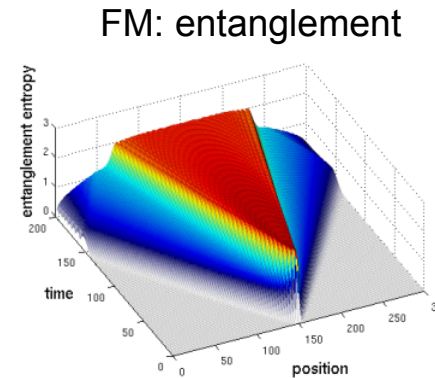
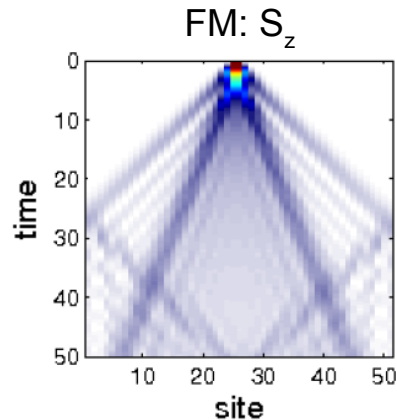
Some real time evolutions (an aside)

- Bound state propagation of a $\uparrow\uparrow$ spin pair in Heisenberg groundstate ($J_z = 1.2$) (Ganahl PRL 2012)
→ dedicated cold atom experiment

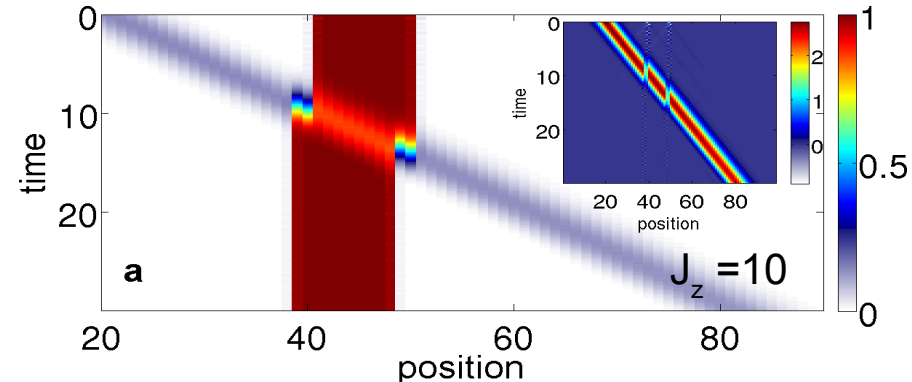
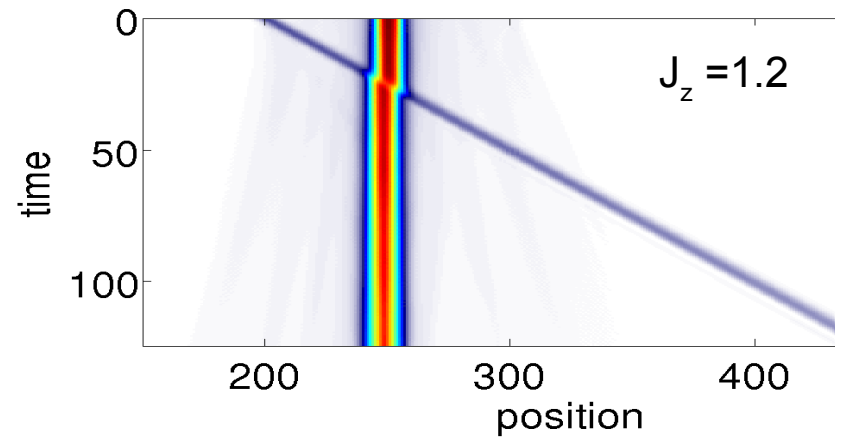


Some real time evolutions (an aside)

- Bound state propagation of a $\uparrow\uparrow$ spin pair in Heisenberg groundstate ($J_z = 1.2$) (Ganahl PRL 2012) \rightarrow dedicated cold atom experiment

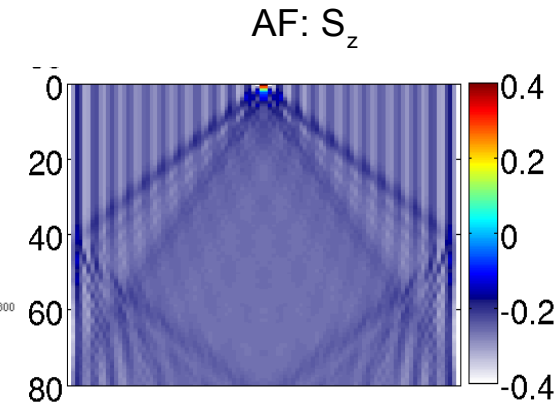
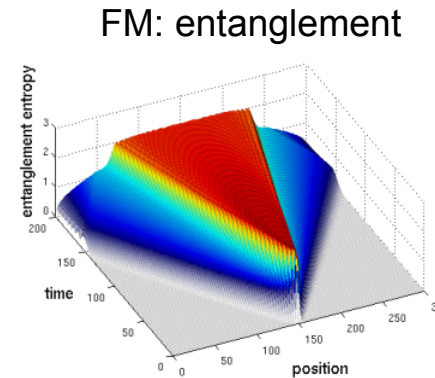
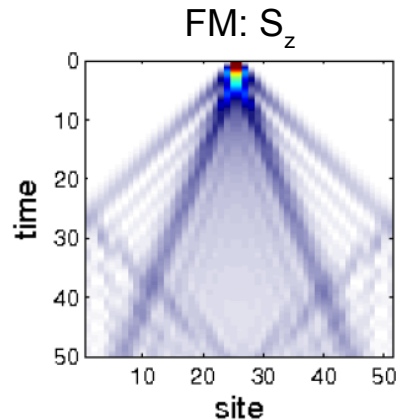


- Scattering between a moving particle and a bound state of 10 particles, which is shifted left by 2 sites (Ganahl 2013) Later reproduced in Bethe ansatz (Vlijm, Ganahl 2015)

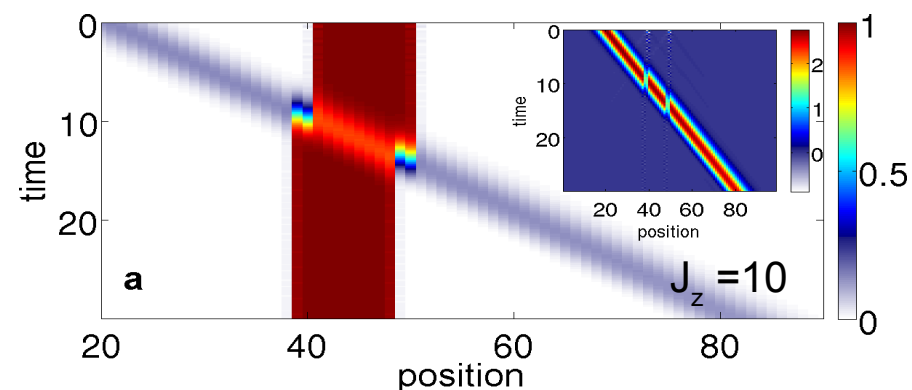
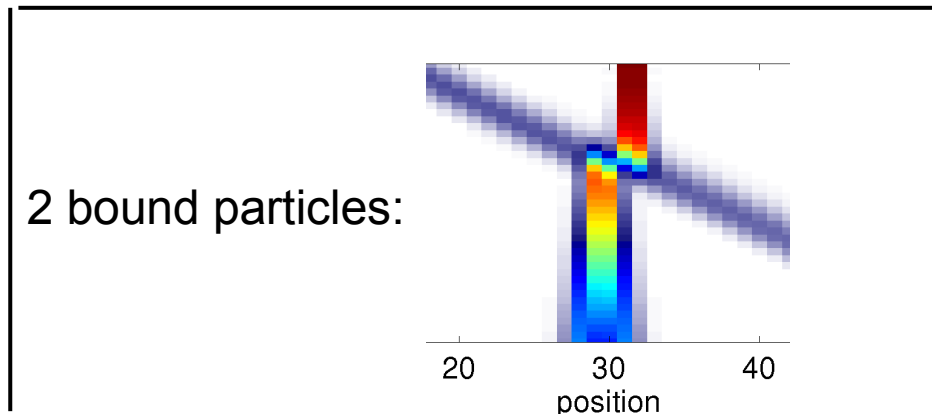
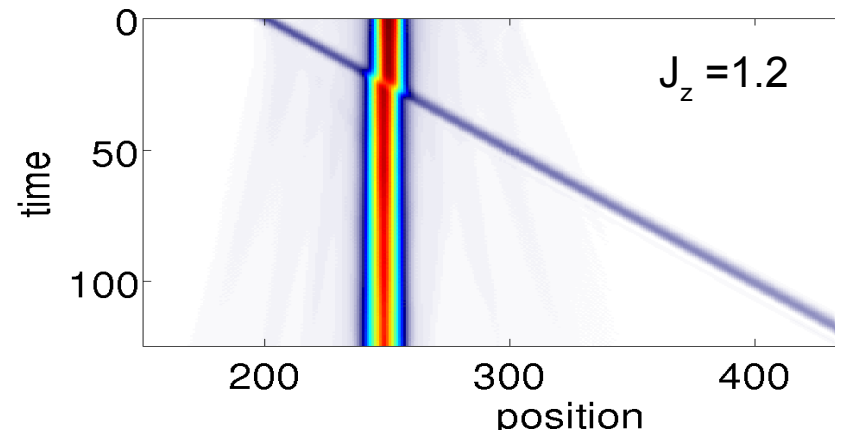


Some real time evolutions (an aside)

- Bound state propagation of a $\uparrow\uparrow$ spin pair in Heisenberg groundstate ($J_z = 1.2$) (Ganahl PRL 2012) \rightarrow dedicated cold atom experiment

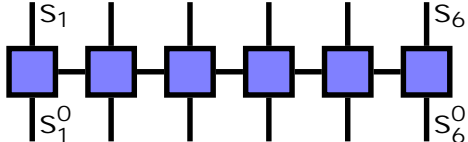


- Scattering between a moving particle and a bound state of 10 particles, which is shifted left by 2 sites (Ganahl 2013) Later reproduced in Bethe ansatz (Vlijm, Ganahl 2015)



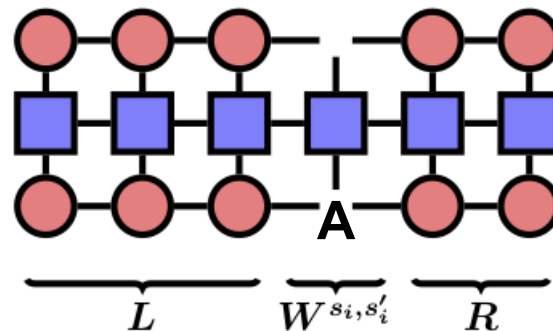
Matrix Product Operators (MPO) and DMRG

- Same approach as for states

$$\hat{O} = \sum_{\{s_i\}, \{s'_i\}} W^{s_1, s'_1} W^{s_2, s'_2} \dots W^{s_L, s'_L} |s'_1, s'_2, \dots, s'_L\rangle \langle s_1, s_2, \dots, s_L|$$


- DMRG: find ground state. Sequentially optimize each MPS matrix A , by finding minimum λ of $H_i^{eff} A^{[i]} = \lambda A^{[i]}$,

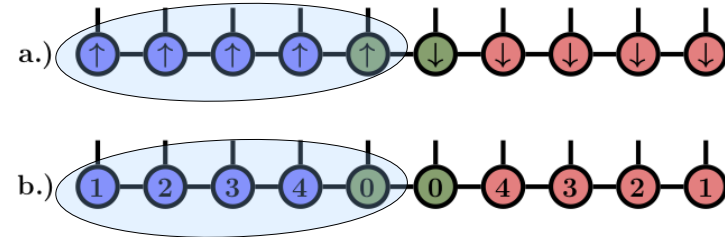
Graphically:



Example: MPO for Anderson Impurity Model

$$H = \sum_{k\sigma} \epsilon_k n_{k\sigma} + \sum_{k\sigma} V_k (c_{0\sigma}^\dagger c_{k\sigma} + h.c.) + \sum_{\sigma} \epsilon_0 n_{0\sigma} + H_{int}$$

- Choose geometry and numbering



- Solution for MPOs (without H_{int})

$$W_{1\uparrow} = (\epsilon_1 n_{1\uparrow} \quad 1 \quad V_1 c_{1\uparrow} \quad V_1 c_{1\uparrow}^\dagger)$$

$$W_{k>1,\uparrow} = \begin{pmatrix} 1 & 0 & 0 & 0 \\ \epsilon_k n_{k\uparrow} & 1 & V_k c_{k\uparrow} & V_k c_{k\uparrow}^\dagger \\ 0 & 0 & p & 0 \\ 0 & 0 & 0 & p \end{pmatrix}$$

with $p = (-1)^n$ for fermion anticommutation

Impurity Solvers

Real time impurity solvers with MPS: strategy

(reminder)

- **To obtain real frequency Green's function:**

- **Ground state** $|\psi_0\rangle$ of impurity model by **DMRG**

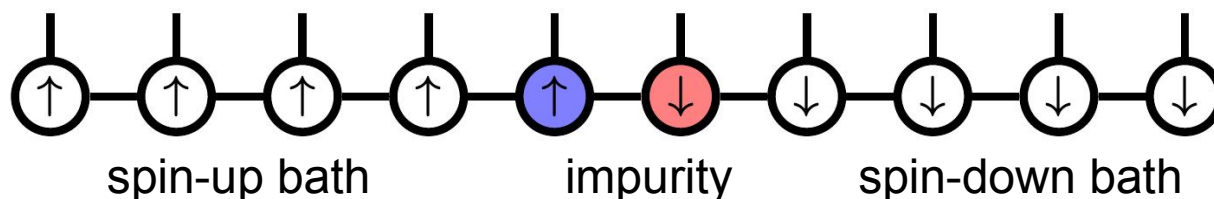
- **Time evolve** excitation: $e^{iHt} c |\psi_0\rangle$ **Real time** \rightarrow small times easiest
 \rightarrow high energies easiest

- Overlap: $G^<(t) = \langle \psi_0 | c^\dagger e^{iHt} c |\psi_0 \rangle$

- “Linear prediction”, Fourier transform $\rightarrow G(\omega)$

One band:

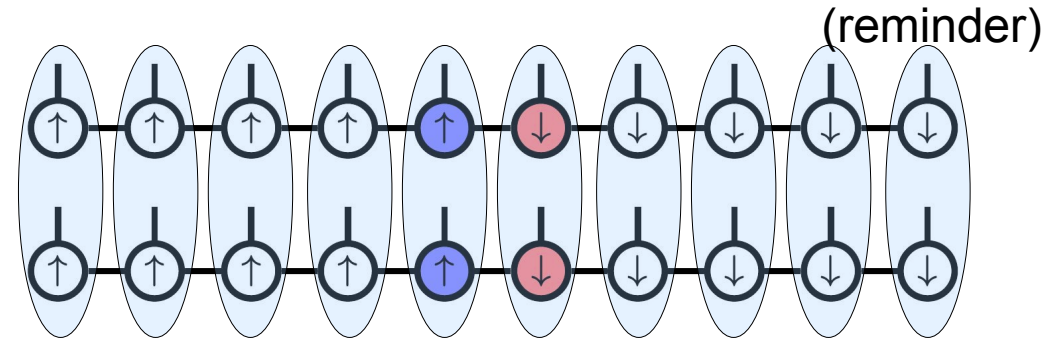
- Separate the spin-up and spin-down baths: (\Rightarrow lower matrix dimensions)



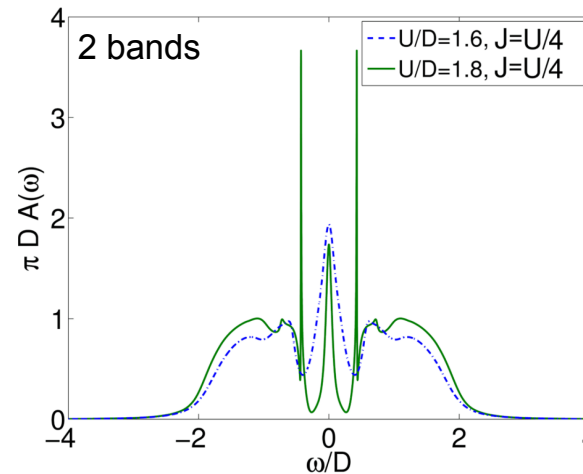
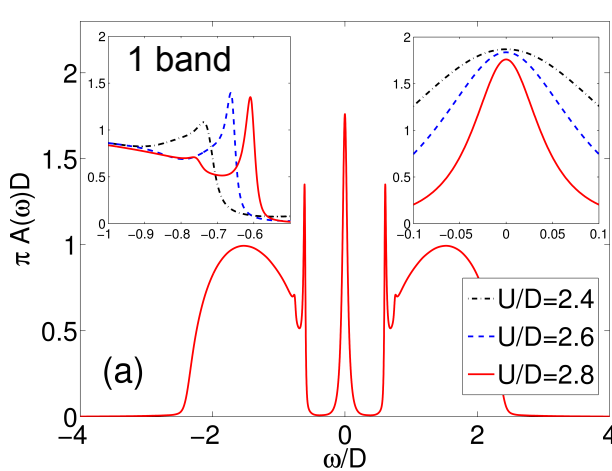
- Large baths ($O(100)$ sites) easily done

Real time impurity Solver with MPS: two bands

- Combine orbitals into bigger sites
- Works very well for 2 bands



- Examples: DMFT spectrum of Hubbard model on Bethe lattice (Ganahl et al, 2015)



Side-peaks: (invisible in QMC):
from interaction of
doublon-holon pairs

(Lee, von Delft, Weichselbaum,
PRL 2017, one-band model)

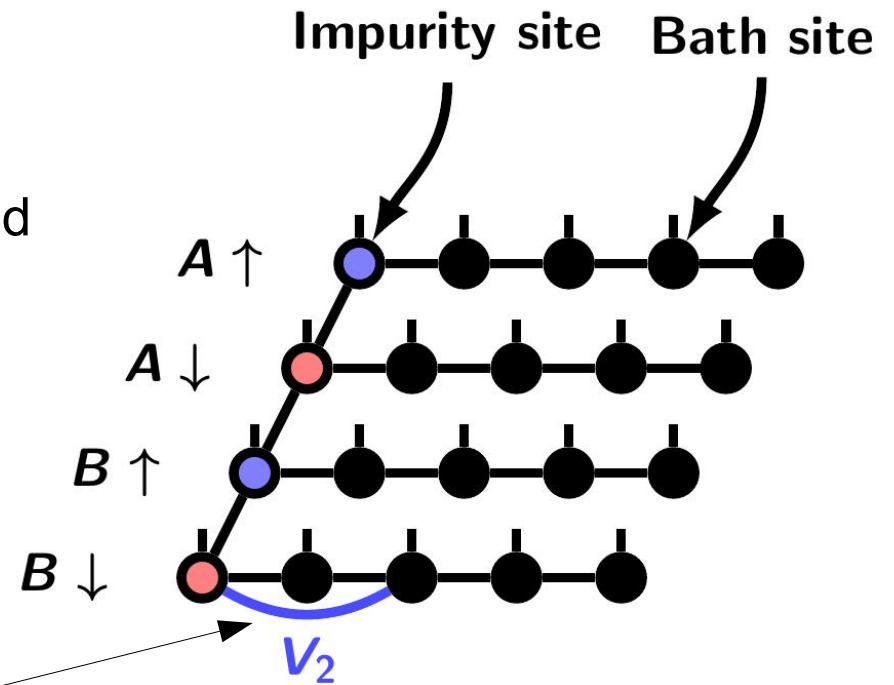
- **Problem:** matrix dimensions m multiply: computational effort $\sim m^3 \times n_{\text{orbital}}$
 \Rightarrow **no more than 2 bands feasible this way**

New approach: Fork Tensor Product States (FTPS)

Bauernfeind 2017, 2018

Example: 2 orbitals A, B:

- **Separate the bands of the bath**
→ small bath matrices
- Tree tensor network, bipartition at any bond
→ **DMRG, Time Evolution** etc. possible
- Tradeoff: Entanglement at impurity
- “**Star geometry**” (no Wilson chains):
→ lower entanglement, much faster



$$V_k \left(c_k^\dagger c_0 + h.c. \right) + \epsilon_k n_k$$

Tree tensor: see also Holzner et al, PRB 2010 (2 orbital NRG)

Kanamori Hamiltonian

$$H = H_{\text{loc}} + H_{\text{bath}} \quad (1)$$

$$H_{\text{loc}} = \epsilon_0 \sum_{m\sigma} n_{m0\sigma} + H_{\text{DD}} + H_{\text{SF}} + H_{\text{PH}}$$

$$H_{\text{DD}} = U \sum_m n_{m0\uparrow} n_{m0\downarrow} + (U - 2J) \sum_{m' > m, \sigma} n_{m0\sigma} n_{m'0\bar{\sigma}} + (U - 3J) \sum_{m' > m, \sigma} n_{m0\sigma} n_{m'0\sigma}$$

$$H_{\text{SF}} = J \sum_{m' > m} \left(c_{m0\uparrow}^\dagger c_{m0\downarrow} c_{m'0\uparrow} c_{m'0\downarrow}^\dagger + \text{h.c.} \right)$$

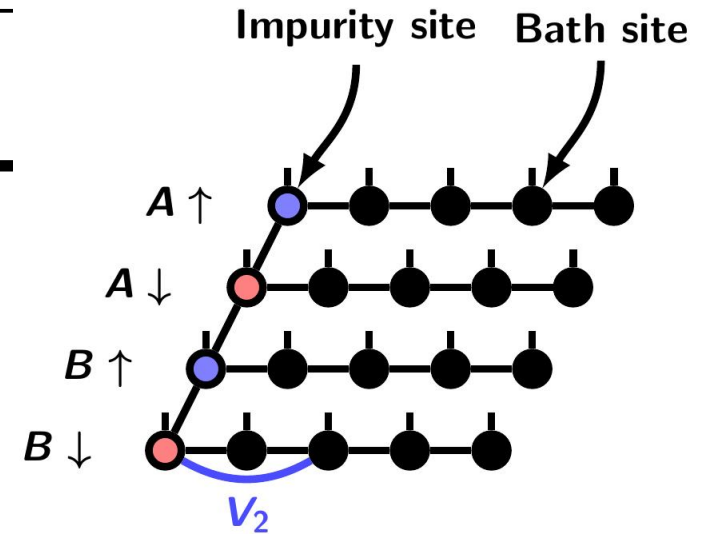
$$H_{\text{PH}} = -J \sum_{m' > m} \left(c_{m0\uparrow}^\dagger c_{m0\downarrow}^\dagger c_{m'0\uparrow} c_{m'0\downarrow} + \text{h.c.} \right)$$

$$H_{\text{bath}} = \sum_{ml\sigma} \epsilon_l n_{ml\sigma} + V_l \left(c_{m0\sigma}^\dagger c_{ml\sigma} + \text{h.c.} \right),$$

$$H_{\text{free}} := H_{\text{bath}} + \epsilon_0 \sum_{m\sigma} n_{m0\sigma} \quad (2)$$

Bath parameters ϵ_l , V_l from **arbitrary discretization** (\leftrightarrow energy resolution) of $\Delta(\omega)$

FTPS: adapt methods



- **SVDs:** combine tensor indices to get matrices → computational effort up to $O(m_I^3 m_B)$,
where m_I : matrix dim. between impurities, m_B : matrix dim. to last bath site)

- **Ground state:** construct MPOs (FTPOs) for H and use **DMRG**

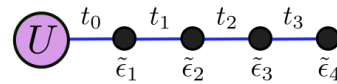
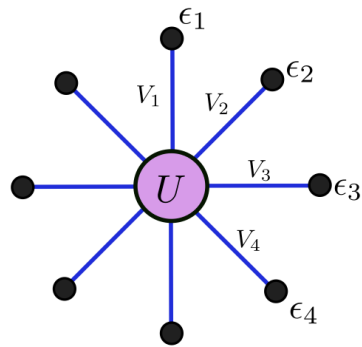
Expensive: $O(m_I^3 m_B^3)$

Time evolution:

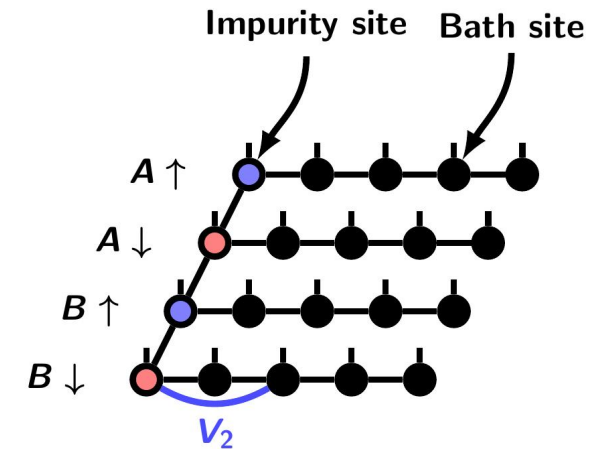
$$e^{-i\Delta t H} \approx \left(\prod_{m' > m} e^{-i\frac{\Delta t}{2} (H_{\text{SF}}^{\text{circled}}_{m,m'} + H_{\text{PH}}^{\text{circled}}_{m,m'})} \right) e^{-i\frac{\Delta t}{2} H_{\text{DD}}^{\text{circled}}} e^{-i\Delta t H_{\text{free}}^{\text{circled}}} e^{-i\frac{\Delta t}{2} H_{\text{DD}}^{\text{circled}}} \left(\prod_{m' > m} e^{-i\frac{\Delta t}{2} (H_{\text{SF}}^{\text{circled}}_{m,m'} + H_{\text{PH}}^{\text{circled}}_{m,m'})} \right)$$

Construct and **apply FTPOs for each time evolution operator** (→ size up to 6 x 10)

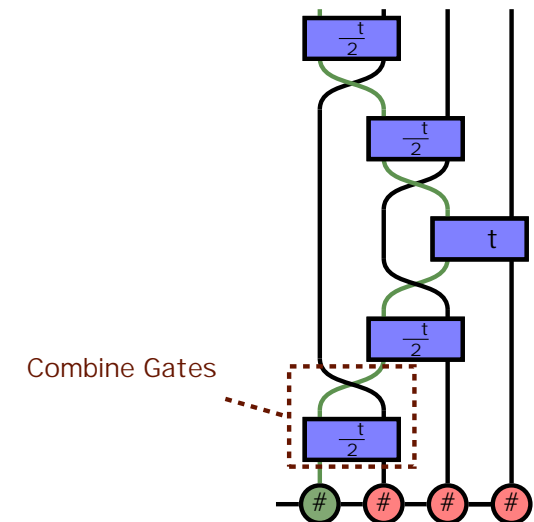
Time evolution of bath



“Star geometry” ↔ Wilson chain



- Use star geometry
- Map onto chain → non-local hoppings (!)
- Treat by “moving impurity through bath and back”
- Achieve much smaller Trotter errors than in Wilson chain:
 - Bath evolution faster by factor 100 for same precision



Results

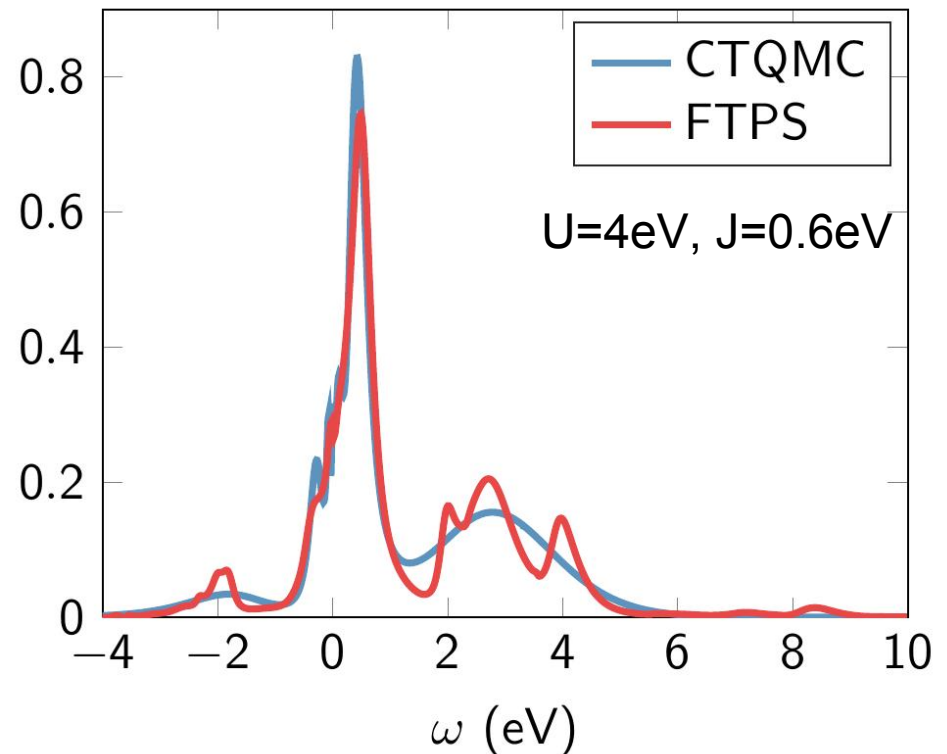
Results: SrVO₃

Phys. Rev. X 7, 031013 (2017)

- 3 band model (t_{2g} subspace), Kanamori-Hamiltonian
 - Large bath (109 bath sites for each orbital-spin combination, converged)
 - Time evolution up to $16eV^{-1}$, $T=0$
 - First: results with only density-density interactions:
-
- Very good agreement with CTQMC (also on imaginary time axis)
 - FTPS only:
3-peak structure in upper Hubbard band

Not resolved by MaxEnt

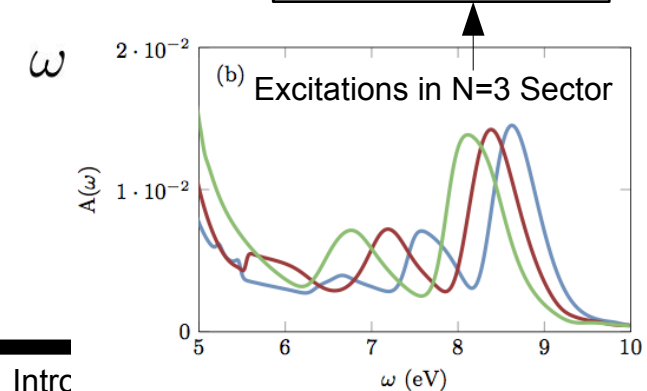
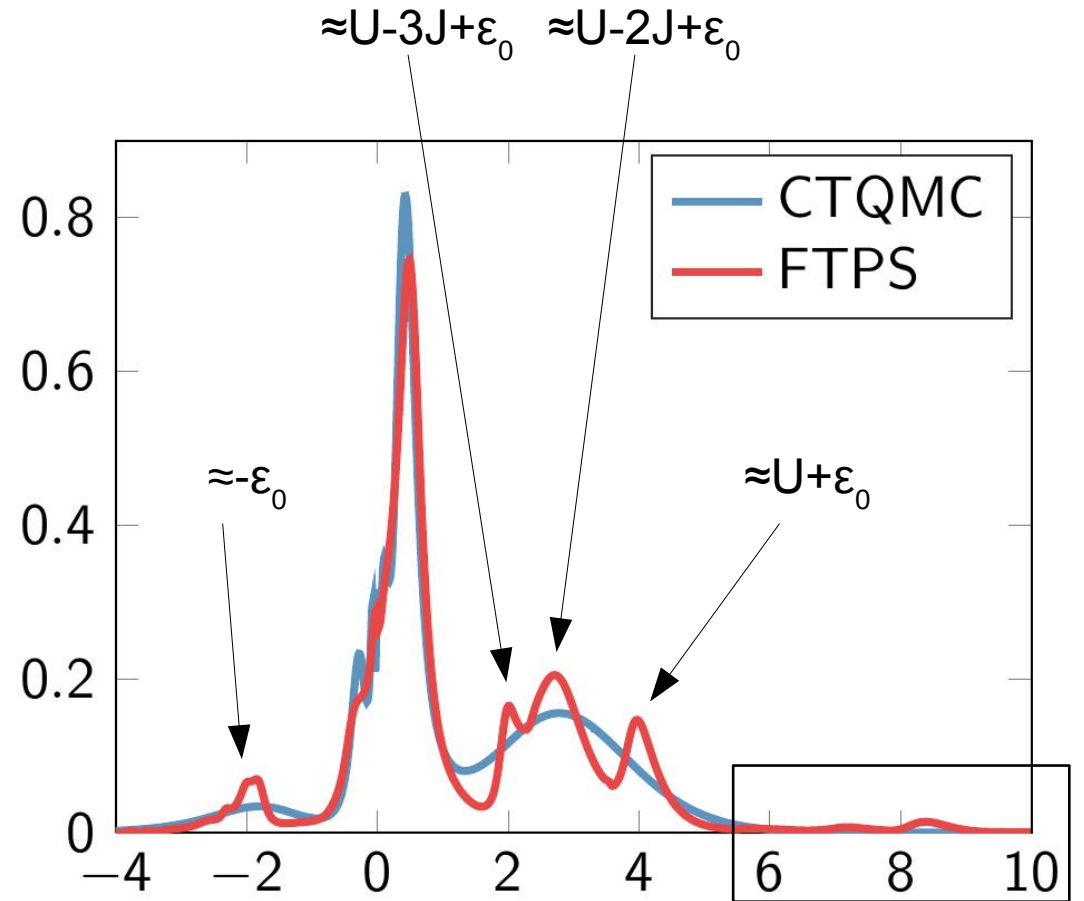
CPU time for one DMFT iteration:
FTPS: 80h, CTQMC: 32h



SrVO₃: multiplet in upper Hubbard band

- FTPS can **resolve multiplets**
- Related to **atomic energies**

particle sector	atomic eigen energies	state
0	ϵ_0	$ 0, 0, 0\rangle$
1	0	$ \uparrow, 0, 0\rangle$
2	$U - 3J + \epsilon_0$	$ \uparrow, \uparrow, 0\rangle$
	$U - 2J + \epsilon_0$	$ \uparrow, \downarrow, 0\rangle$
	$U + \epsilon_0$	$ \uparrow\downarrow, 0, 0\rangle$
3	$3U - 9J + 2\epsilon_0$	$ \uparrow, \uparrow, \uparrow\rangle$
	$3U - 7J + 2\epsilon_0$	$ \uparrow, \uparrow, \downarrow\rangle$
	$3U - 5J + 2\epsilon_0$	$ \uparrow\downarrow, \uparrow, 0\rangle$



SrVO₃: upper Hubbard band for different J

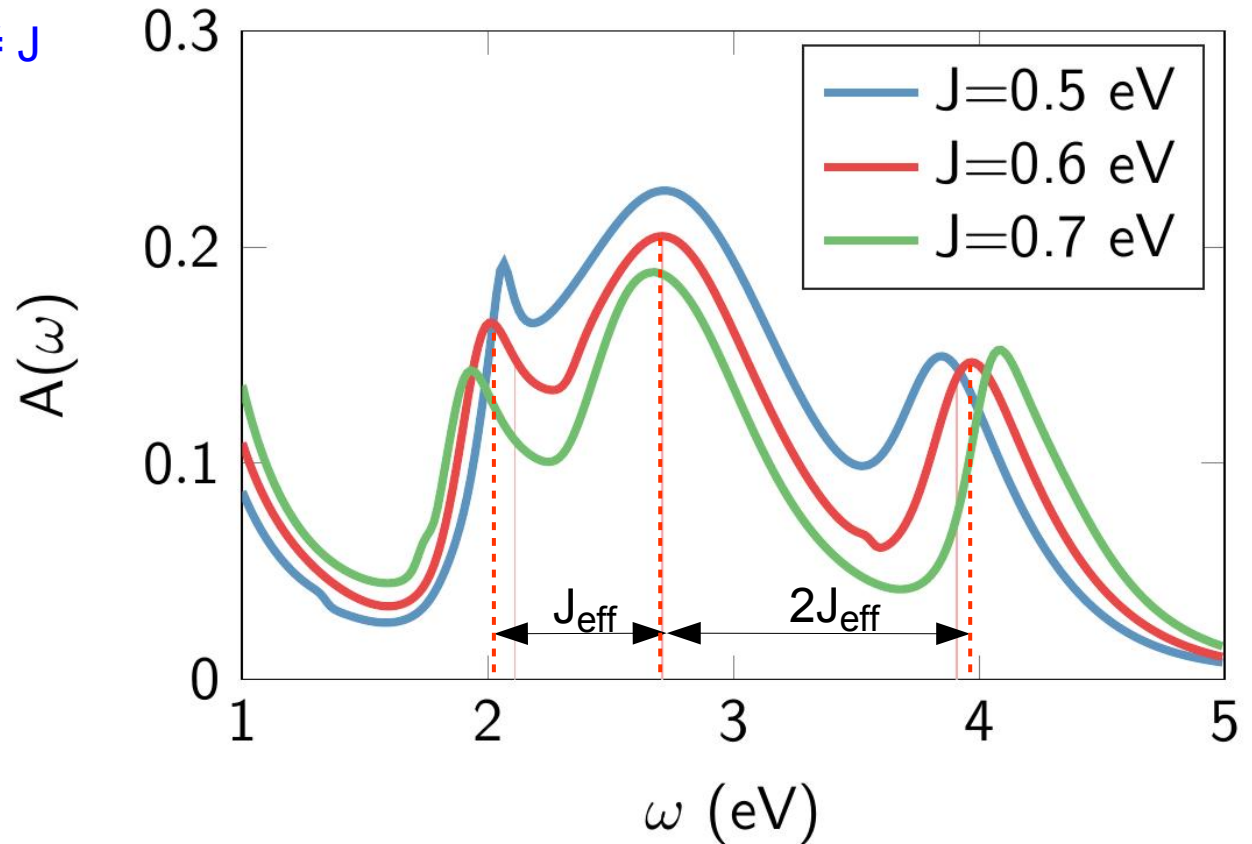
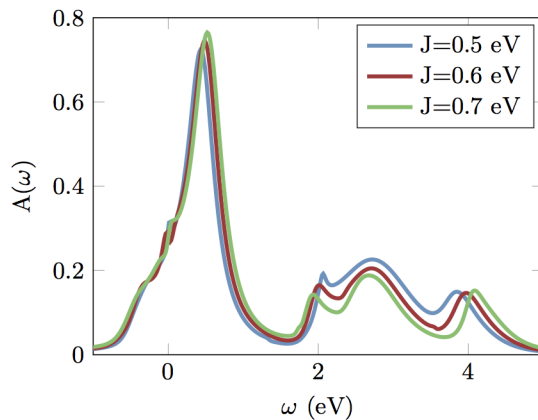
- Interactions \Rightarrow broadened and shifted peaks
- Can be described by effective $J_{\text{eff}} \neq J$

$$J = 0.5 \text{ eV} \rightarrow J_{\text{eff}} = 0.59(6) \text{ eV}$$

$$J = 0.6 \text{ eV} \rightarrow J_{\text{eff}} = 0.66(3) \text{ eV}$$

$$J = 0.7 \text{ eV} \rightarrow J_{\text{eff}} = 0.72(2) \text{ eV}$$

- Central peak almost constant



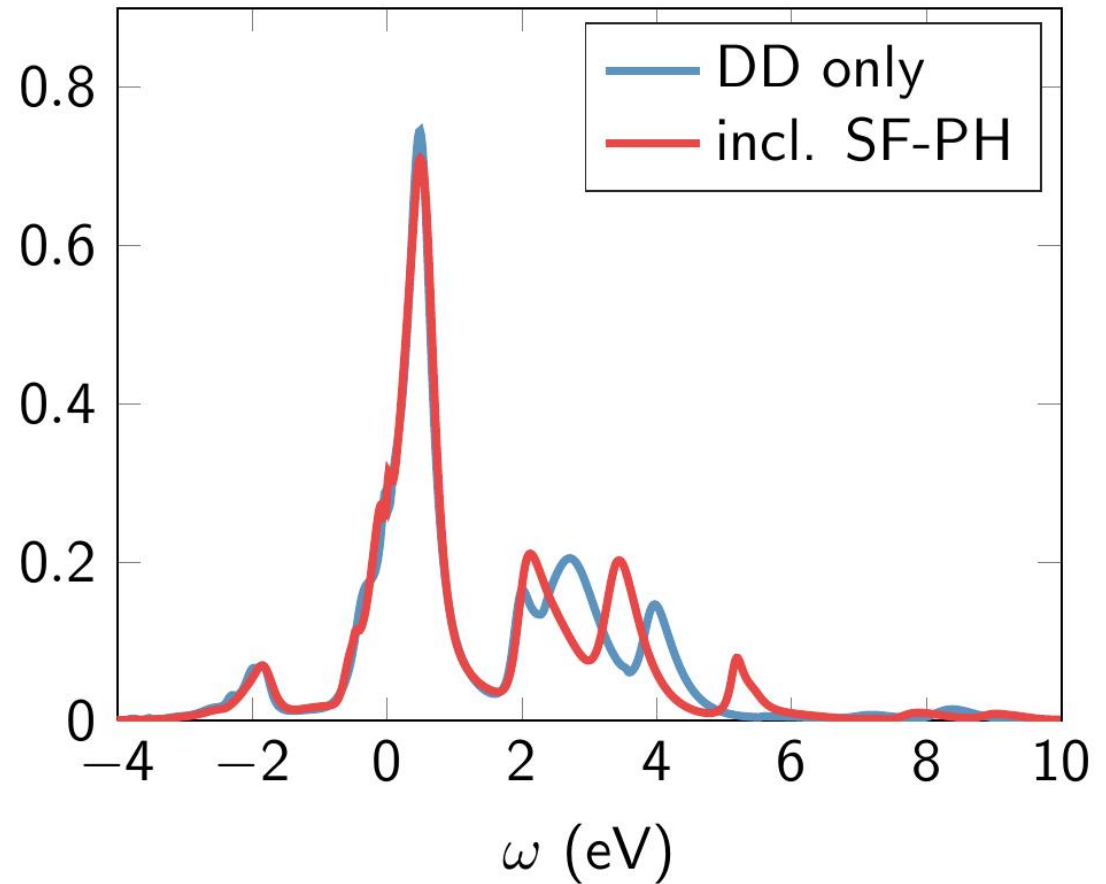
SrVO₃: full rotational symmetry

Include spin flip and pair hoppings

Only affect N=2 sector →
Hole excitation and quasi particle
peak do not change

Different multiplets due to different
atomic eigenstates/eigenenergies.

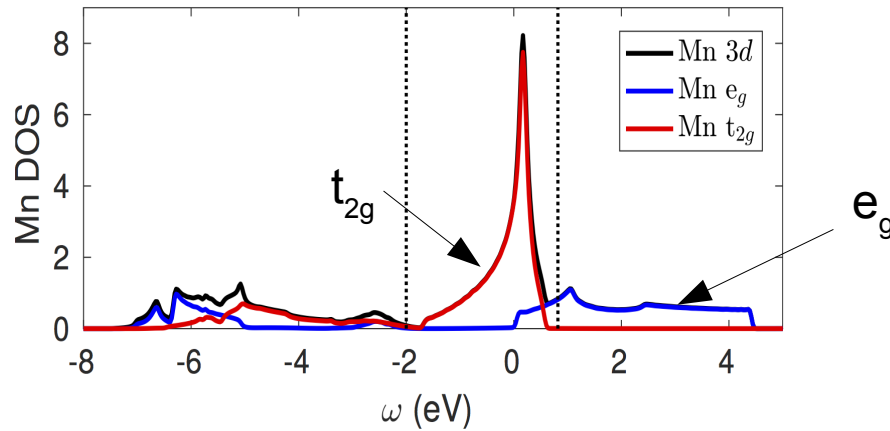
Energy differences **2J** and **3J**



SrMnO₃

- 3 electrons in Mn-3d orbitals. Mott Insulator with $|GS\rangle \approx |\uparrow, \uparrow, \uparrow\rangle + |\downarrow, \downarrow, \downarrow\rangle$

- DFT-DOS:

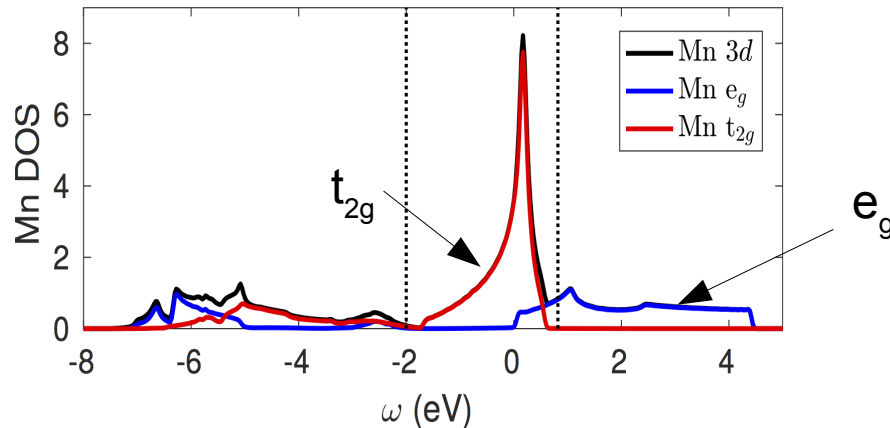


- e_g orbitals largely above E_F → “unoccupied”
Is e_g important ?

SrMnO₃

- 3 electrons in Mn-3d orbitals. Mott Insulator with $|GS\rangle \approx |\uparrow, \uparrow, \uparrow\rangle + |\downarrow, \downarrow, \downarrow\rangle$

- **DFT-DOS:**



- e_g orbitals largely above $E_F \rightarrow$ “unoccupied”

Is e_g important ?

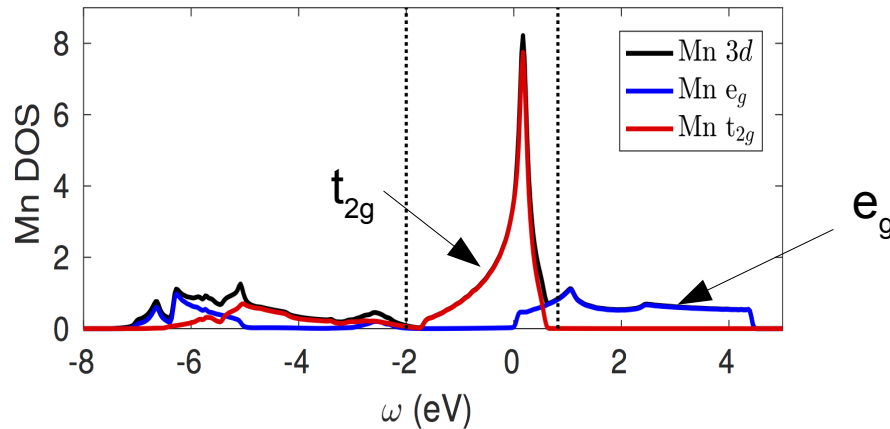
- Strong hybridizations with oxygen p-states in lower Hubbard band

\rightarrow Use wide energy window [-10eV, 5eV]
for Wannier projection
GS then mixes N=3 and N=4 sectors

SrMnO₃

- 3 electrons in Mn-3d orbitals. Mott Insulator with $|GS\rangle \approx |\uparrow, \uparrow, \uparrow\rangle + |\downarrow, \downarrow, \downarrow\rangle$

- **DFT-DOS:**

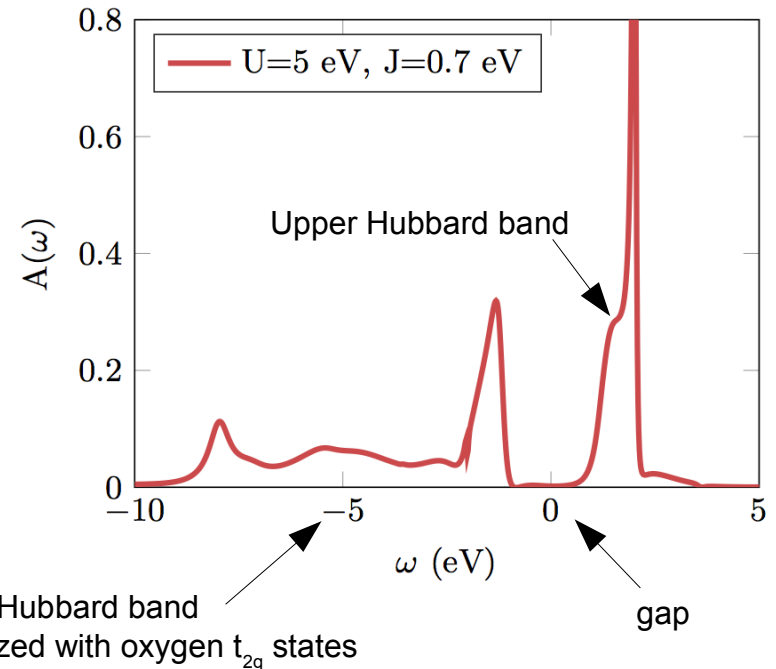


- e_g orbitals largely above $E_F \rightarrow$ “unoccupied”
Is e_g important ?

- Strong hybridizations with oxygen p-states in lower Hubbard band

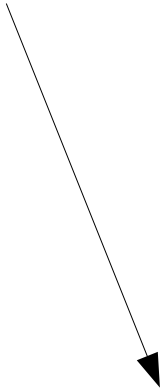
\rightarrow Use wide energy window [-10eV, 5eV] for Wannier projection
GS then mixes N=3 and N=4 sectors

DMFT: t_{2g} only

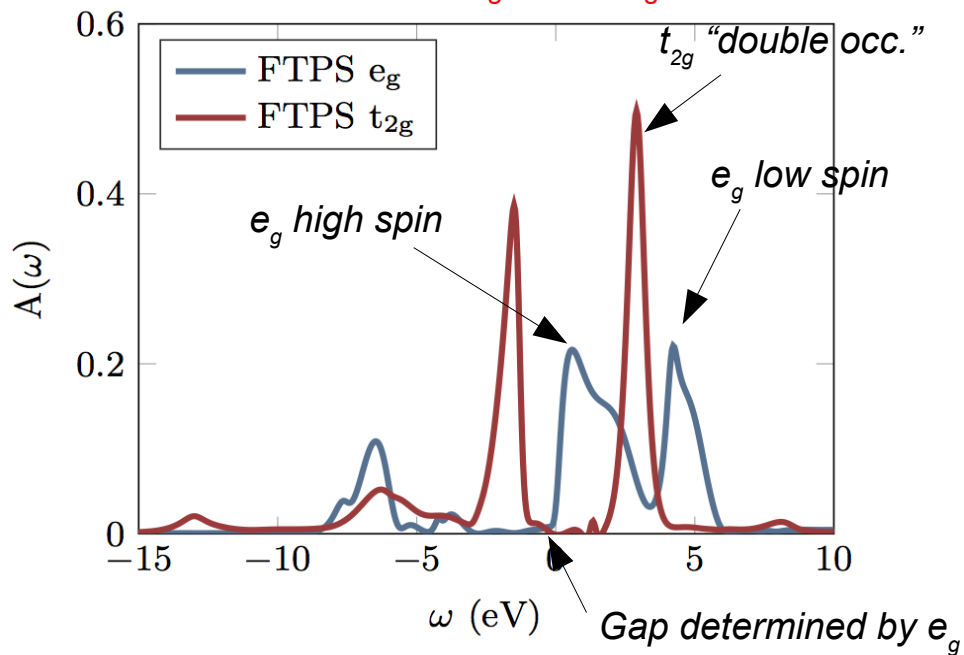


SrMnO₃: t_{2g} and e_g orbitals

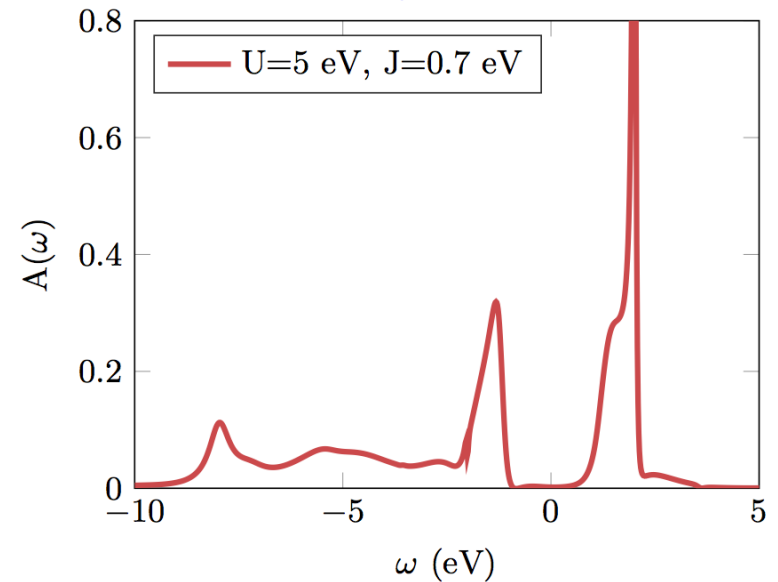
- Full 5-band calculation ($U=6.0$, $J=0.8$)



DMFT: t_{2g} plus e_g

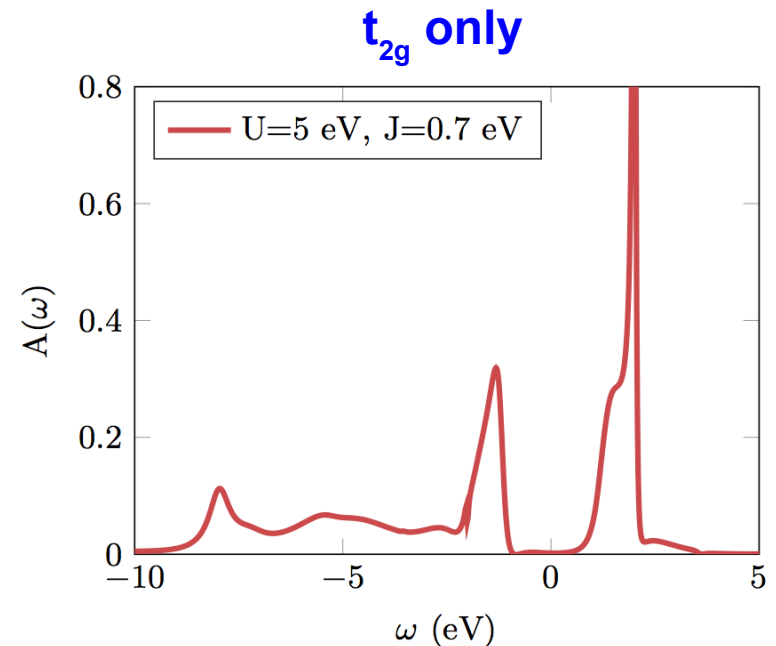
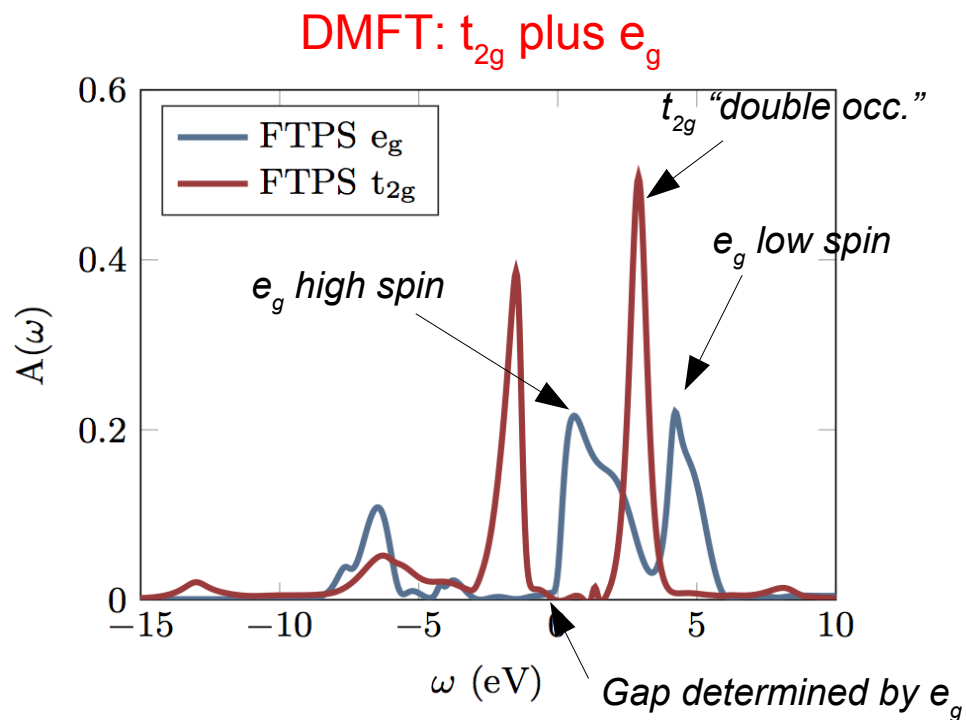


t_{2g} only



SrMnO₃: t_{2g} and e_g orbitals

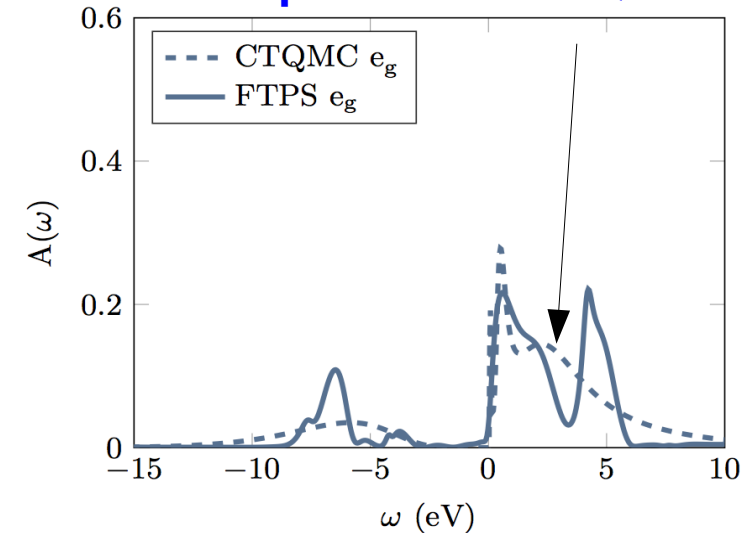
- Full 5-band calculation ($U=6.0$, $J=0.8$)
- e_g is important:
 - determines the gap
 - creates 3-peak structure above E_F



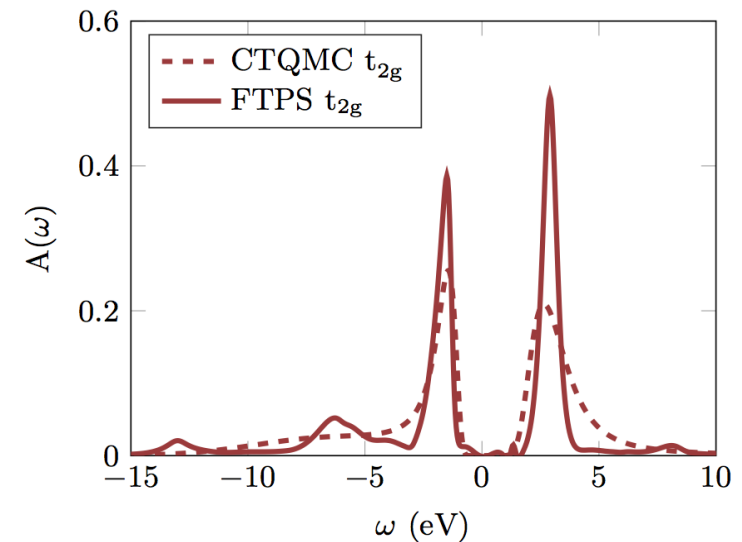
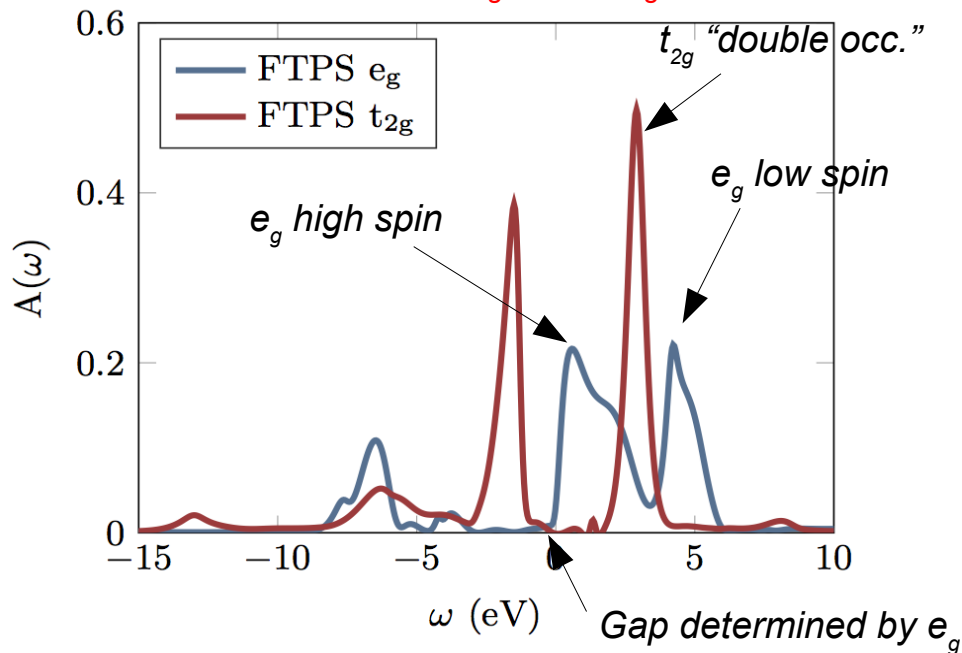
SrMnO₃: t_{2g} and e_g orbitals

- Full 5-band calculation ($U=6.0$, $J=0.8$)
- e_g is important:
 - determines the gap
 - creates 3-peak structure above E_F (not resolved by CTQMC)

Comparison to CTQMC



DMFT: t_{2g} plus e_g



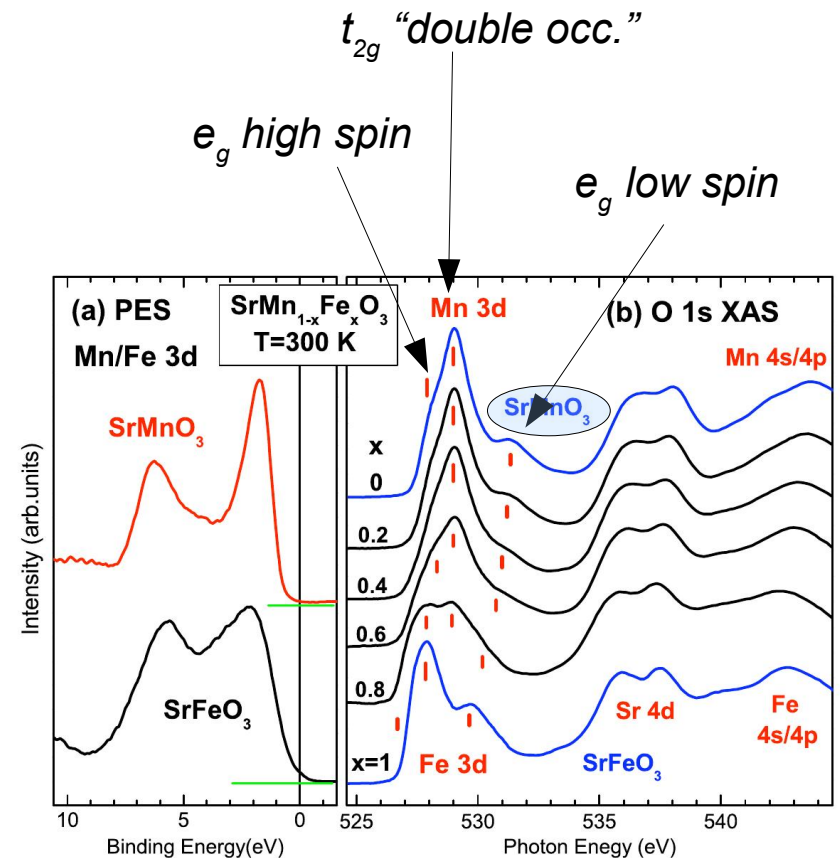
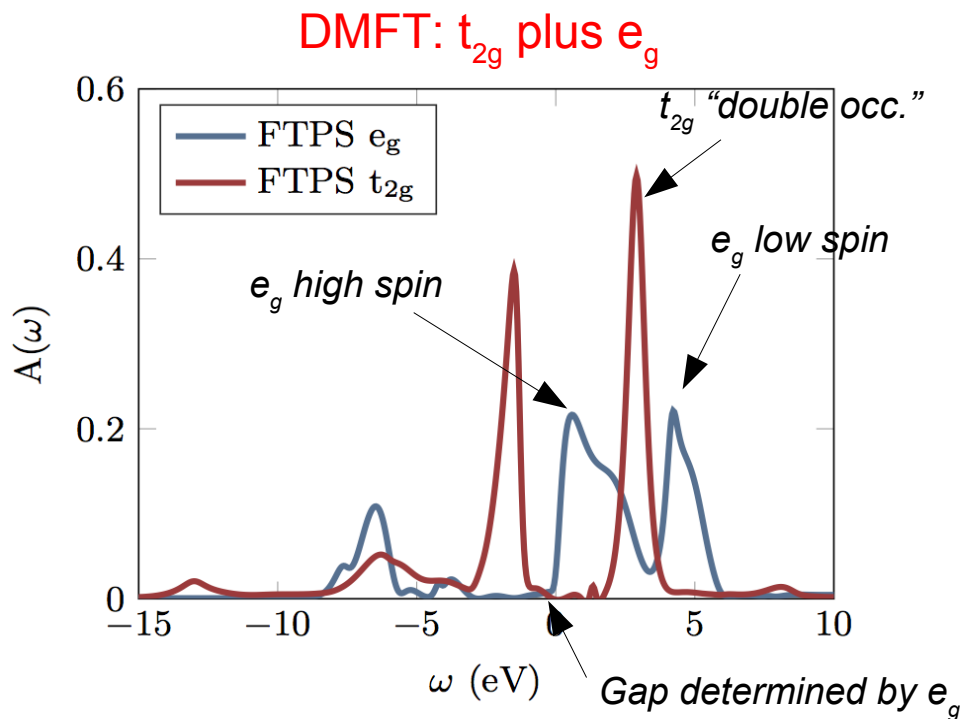
FTPS: 700 CPU-h, CTQMC: 600 CPU-h

SrMnO₃: t_{2g} and e_g orbitals

- Full 5-band calculation ($U=6.0, J=0.8$)
- e_g is important:
 - determines the gap
 - creates 3-peak structure above E_F (not resolved by CTQMC)

Comparison to experiment

3-peak structure visible in experiment



J.-S. Kang et al.,
PRB 78, 054434 (2008)

Conclusions

- **FTPS: real time impurity solver for DMFT**
 - Efficient: comparable to CTQMC
 - $T=0$
 - Large baths, no analytic continuation → high resolution at all energies
 - 5-orbital calculations possible
 - Can resolve multiplets in upper Hubbard band
SrMnO₃: three-peak structure $e_g t_{2g} e_g$ is also visible in experiment
- **Outlook:**
 - Non-diagonal baths, without sign problem (in preparation)
 - Nonequilibrium (in preparation) → next talk by Martin Eckstein
 - Better resolution than CT-QMC even at low energies (25meV) (→ M. Rumetshofer)
- **Limitations:**
 - Single site (so far)
 - No black box yet
 -

